South African Journal of Chemical Engineering 41 (2022) 111–128

Contents lists available at ScienceDirect

South African Journal of Chemical Engineering

journal homepage: www.elsevier.com/locate/sajce

To DoE or not to DoE? A Technical Review on & Roadmap for Optimisation of Carbonaceous Adsorbents and Adsorption Processes

Mikhail Gorbounov, Jess Taylor, Ben Petrovic, Salman Masoudi Soltani *

Department of Chemical Engineering, Brunel University London, Uxbridge UB8 3PH, UK

ARTICLE INFO

Key words:
Activation
Adsorbent
Adsorption
Carbon
Design of Experiments
DoE
Optimisation

ABSTRACT

Design of experiment (DoE) techniques are invaluable tools which readily allow for efficient optimisation of processes *via* simultaneous evaluation of a combination of input parameters. Such approaches can yield positive outcomes whilst minimising the number of resources and amount of time utilised, hence, achieving a more robust approach. Additionally, when designing the experiment intelligently information about the interaction between the variables could be gathered, therefore, allowing for a more in-depth understanding of the process and identification of the "key players". This method of conducting an experimental campaign is, unfortunately, underused (or often misused) in academia. This review aims to technically scrutinise the employment of design of experiment techniques in the context of synthesis and deployment of carbonaceous sorbents and the optimisation of the adsorption processes in both gaseous and aqueous media for environmental applications. We have also discussed how the implementation of DoE techniques in interpreting the results and the underlying trends and/or adsorption mechanisms could help with a better understanding of such observations. Additionally, a brief description of the most popular experimental design techniques with an explanation and a simple visualisation is provided. This review aims to facilitate a greater understanding and appreciation of these powerful optimisation tools, and to depict the best practices upon their employment in academic research in the field of chemical and environmental engineering.

1. Introduction

"Time is of the essence". This aphorism is used plentifully with a recent example being provided by the speed of development and rollout of various COVID-19 vaccines in 2021. Such a pressing issue had to be resolved quickly, efficiently and without damaging the quality of the final product. An industrial solution to overcome time limitations and other (financial or resource) constraints is implementation of advanced experimental designs to optimise the manufacturing processes in a more sustainable way. Science can be viewed as a *production line* for information and knowledge, and therefore, in order to optimise the process of "science generation", statistical techniques - typically referred to as design of experiments (DoE) - can be employed in the same way as they are used to address optimisation challenges in an industrial setting. An intuitive method for conducting a typical experimental campaign to reveal the impact of a select variable on a target output, is the one-factor-at-a-time (OFAT) approach. This conventional pathway relies upon changing one of the parameters, while keeping the others constant. However, this technique does not identify possible interactions between the studied factors, thereby, compromising the true optimum point. An advanced design, however, reveals the hidden impacts of simultaneous change of variables as well as provides an additional benefit of reduction of the number of experiments needed to complete an experimental campaign. (Smallwood, 1947) defined design of experiments as "planning of a number of experiments in order for their combined result to yield a maximum amount of information", hence, an appropriate DoE has to be painstakingly devised prior to the conduction of experiments. There are myriad advanced designs with an aim to either optimise time and/or resources. These designs, however, must generate suitable "responses" to enable improvement of the process.

Despite such key benefits, the employment of DoE appears to have been significantly overlooked in academia (Snetsinger and Alkhatib, 2018). Nevertheless, despite the frequent use of "optimisation" in the title of peer-reviewed publications, only 6.67 % of articles published in Analytica Chimica Acta in 2009 have identified the optimum operating envelopes through the employment of a non-OFAT multivariable approach (Leardi, 2009). In 2020, however, the number of papers published in the Journal of Hazardous Materials, claiming adsorption/adsorbent optimisation, and employing a DoE, was raised by

* Corresponding author: +44-(0)1895 265884.
E-mail address: Salman.MasoudiSoltani@brunel.ac.uk (S. Masoudi Soltani).

https://doi.org/10.1016/j.sajce.2022.06.001
Received 1 January 2022; Received in revised form 6 May 2022; Accepted 3 June 2022
Available online 6 June 2022

Nomenclature

AC	Activated Carbon
ACF	Activated Carbon Fibre
T_{act}	Activation Temperature
τ_{act}	Activation Time (often referred to as dwell(ing) time or hold(ing) time)
T_{ads}	Adsorption Temperature
τ_{ads}	Adsorption Time
ANOVA	Analysis Of Variance
BBD	Box-Behnken Design
BG	Brilliant Green
S_{BET}	Brunauer–Emmett–Teller Surface Area
CCD	Central Composite Designs
VTSA	combined Vacuum and Thermal Swing Adsorption
DoE	Design of Experiments
D	Desirability
X_N	Factor N (often referred to as parameter or variable)
F-value	Fisher value
IR	Impregnation Ratio of precursor to activation (ing) agent
ID	Inner Diameter
$X_N X_M$	Interaction between factor N and factor M
MG	Malachite Green
MB	Methylene Blue
MWCNT	Multi-Walled Carbon Nanotubes
OFAT	One-Factor-At-a-Time
PSA	Pressure Swing Adsorption
p-value	Probability Value
Y	Response
RSM	Response Surface Methodology
S/N	Signal-to-Noise ratio
SSA	Specific Surface Area
TSA	Temperature Swing Adsorption
VOC	Volatile Organic Compound

approximately 28.5%. This could be due to adsorption (in aqueous media mainly) being a fairly mature technology, and hence, having received a higher attention in terms of industrial optimisation *via* DoE techniques. Nevertheless, the value of optimisation of an adsorption process cannot be understated. Since the main challenges associated with optimisation of both the synthesis protocol and the application of carbonaceous adsorbents are derived from the vast range of precursors, modification/processing methods as well as the envisaged separation technique and adsorbate species (i.e. the adsorbate itself, its concentration, competing adsorption, process conditions and etc). Thus, the optimisation of (e.g.) *an activated carbon derived from coconut shell by physical activation with steam for the purposes of hydrogen separation in a vacuum swing adsorption process of a steam-methane reforming setup* would greatly differ from (e.g.) *tailoring chemically a recycled carbon nanofibre to be employed in a water-treatment facility for purification from antibiotics for aquaculture purposes*. Not only the impactful factors but also their appropriate levels change significantly when substituting each and any part of a given process with an alternative approach. Having this said, activation temperature (T_{act}) and time (τ_{act}) are often considered for evaluation (alongside the impregnation ratio (IR) of precursor to activation agent if dealing with a chemical activation approach), whereas adsorption temperature (T_{ads}) and adsorption time (τ_{ads}) are often chosen as the input variables if optimising the separation process. The response variables, on the other hand, are quite often chosen to be: product yield, adsorption capacity of the material (or other modes of quantifying surface area (e.g. various morphological properties or "*indicator*" numbers) to serve as an estimation) as well as operating/production cost or a combination of them. Moreover, in order to be viable, these optimisation campaigns should be carried out utilising the minimum number of resources, both monetary and natural, thus, highlighting the value of advanced experimental designs.

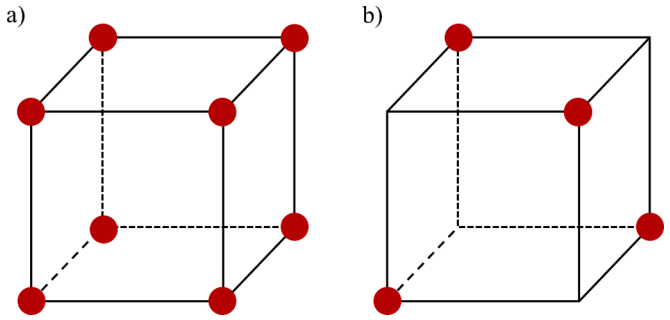

Fig. 1. – 2^3 factorial design space: a) Full factorial; b) Fractional factorial.

In this work, we have rigorously reviewed the employment of the key DoE techniques in the synthesis and application of various carbonaceous adsorbents by carefully scrutinising the scientific literature. The limited number of available papers reviewed in this work is a clear indication of the visible gap in this research area and the room for further improvement. Ultimately, this review paper aims to popularise and propagate deployment of such powerful optimisation tools in synthesis and application of carbonaceous adsorbents for environmental technologies. The main search engine to conduct this review was Scopus to blanket the most impactful publications in the scientific literature.

The following section of the paper is designed to introduce the reader to the most common DoE tools and methods, their most appropriate applications, merits and limitations as well as best practices. Within this chapter a brief description of the most commonly employed statistical analysis techniques is also provided. Next, optimisation of the syntheses processes of various carbonaceous adsorbents is presented; describing the influence of the parameters at the evaluated levels (i.e. conditions) employed (as well as their interactions) and their output, on the target dependent variable. This chapter is divided into subcategories which are based on the target variable (parameters) that have been optimised. Furthermore, this section includes a discussion of the underlying scientific reasoning together with brief critiques of the experimental designs at hand. In section 0, especial attention has been given to the optimisation of the adsorption processes with the help of DoE. Similarly, the observations are confirmed with a description of the impacts and relationships identified in the literature among the input process variables and their interactions on the desired responses. The latter portion of this review paper provides a roadmap for practitioners in this realm of research.

2. Common Experimental Designs and Statistical Analysis Techniques

This section explores the most common DoE matrices used for adsorbent optimisation as well as the analytical techniques used in data interpretation. The choice of the technique is dependent on the desired outcome, namely, *to screen a number of variables to identify the most impactful ones*, or *to optimise the procedure and visualise (map) the response surface*. Factorial designs generally favour the former objective, whereas the latter is normally accomplished by other DoE matrices. Nevertheless, the scientific literature is populated with research where such techniques have been deployed interchangeably.

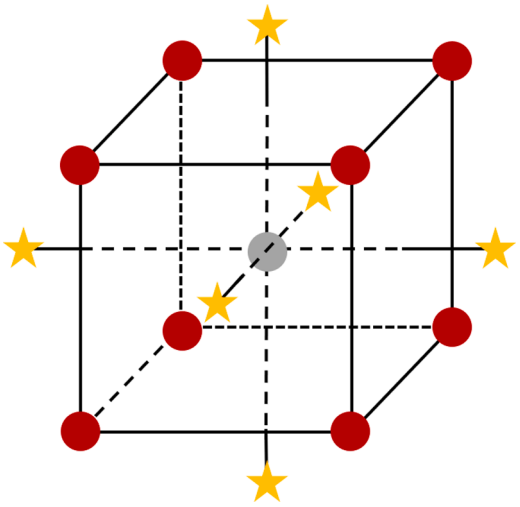

Fig. 2. – Central composite design space.

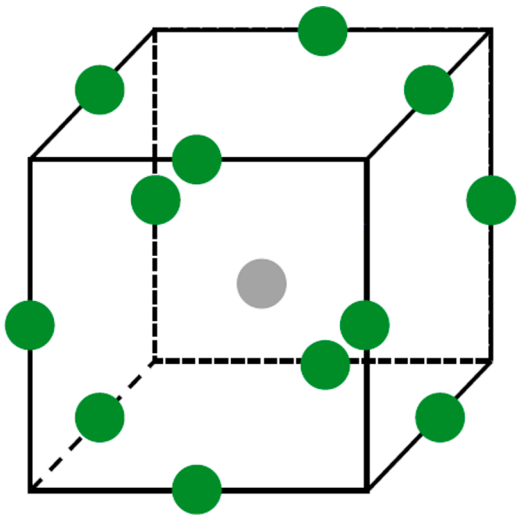

Fig. 3. – Box-Behnken design space.

2.1. Factorial DoE

Factorial DoEs are preferable for initial (screening) studies and exist in a variety of forms. When the number of parameters is *moderate*, a full factorial design may be feasible, and render to be the most accurate. Such matrices aim to evaluate all possible combinations; thus, the number of experiments (*N*) can be calculated *via*:

$$N = L^P \tag{1}$$

Where *L* is the amount of investigated levels and *P* is the number of input factors (parameters). Often, this design is implemented in an investigation of 3 input variables at 2 different levels each resulting in 8 factorial points (i.e. experimental conditions) as shown in Fig. 1a. However, when evaluating a larger number of parameters, fractional factorial designs may be preferable. This "variation on the full factorial DoE" reduces the number of trials needed for the experimental campaign by focusing only on the main effects and interactions. Such designs also provide great efficiency for screening studies or when evaluating a larger number of parameters. Both of these DoE matrices can be easily depicted as cubes. Fig. 1b provides a visualisation of the same 2^3 factorial design as described above (and pictured in Fig. 1a), though in form of a ½ fraction design.

Another DoE method discussed in this paper is the Placket-Burman design. This technique is often utilised as a preliminary screening tool to determine factors with significant contribution in the early experimentation phase. The method is usually only applied when there is a lack of knowledge about the system in question. An important limitation of the Placket-Burman design is that the main effects can be strongly skewed due to any existing interactions between the factors.

2.2. Central Composite DoE

Classically, if the task at hand requires response optimisation, or mapping out the design space for the dependent variable, Central Composite designs (CCD) could be employed. The latter objective is a significant part of the Response Surface Methodology (RSM). RSM is a valuable tool used to improve/optimise and/or find the frailties of the process, which is discussed at length in Section 2.5.

CCD is a useful method due to the superior ability in estimating curvature and, therefore, should be used when a linear model fails to accurately represent the design space. As introduced by (Box and Wilson, 1951), the design features the fractional factorial design points ([+1] and [-1]), *i.e.* experimental conditions. Axial (often referred to as "star") points ([+α] and [-α]) and centre points such that the number of tests, N, can be determined as:

$$N = 2^k + 2k + N_0 \tag{2}$$

where 2^k, $2k$ and N_0 refer to the number of factorial, axial and central points, respectively. For a design with two variables, nine experiments must be defined (if $N_0 = 1$) within the range of variables in order to allow development of a second-order polynomial that can be used to predict the response:

$$y = \beta_0 + \beta_1 x_1 + \beta_2 x_2 + \beta_3 x_3 + \beta_{11} x_1^2 + \beta_{22} x_2^2 + \beta_{33} x_3^2 + \beta_{12} x_1 x_2 + \beta_{13} x_1 x_3 + \beta_{23} x_2 x_3 \tag{3}$$

where *y* is the predicted response, (β_0), (β_1, β_2, β_3), (β_{12}, β_{13}, β_{23}), and (β_{11}, β_{22}, β_{33}) represent intercept, linear, interaction, and quadratic coefficients, respectively. Thus, a CCD contains within its design an ever-present factorial design. Therefore, if it is evident that a factorial (regardless full or fractional) DoE does not suffice for appropriate modelling of the process being optimised, furthering the investigation by incorporating the performed design into a wider CCD framework is a viable solution. This overlay can be easily visualised from Fig. 2, where the red dots represent the ever-present factorial design points, the yellow stars represent the axial (or star) points and the grey circle in the middle stands for the centre point experiment (in this visualisation, no repetitions are shown).

Additionally, the star points in the CCD allow the user to glimpse outside of the original matrix, hence, broadening the design space as well as the response surface.

2.3. Box-Behnken DoE

A Box-Behnken design (BBD) is considered to be a more efficient alternative to CCD (Alaoui et al., 2015), (Ferreira et al., 2007) (especially when working with a high number of factors) as they normally require less runs to complete an experimental campaign. Thus, CCD is usually chosen over BBD when three or less factors are being considered as the former designs are more flexible with respect to two-way interactions. However, when working with three factors, BBD does not comply with the criteria for iso-variance per rotation, meaning that the design cannot be rotated around its centre point without changing the prediction of variance. This can be attributed to the positioning of the design points within the subareas of the dimension, centre points must be added to maintain rotatability in these cases (as can be seen from Fig. 3).

BBD makes use of the following expression to identify the number of

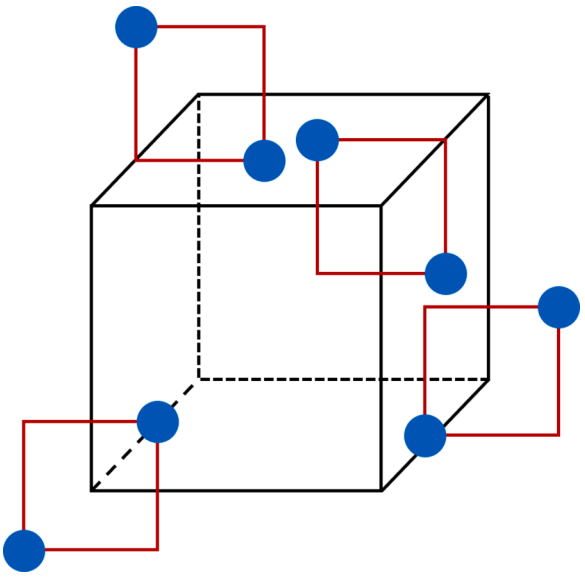

Fig. 4. – 2^5 Taguchi design space.

experiments required to design the response surface:

$$N = 2P(P-1) + N_0 \tag{4}$$

where P represents the number of parameters (factors) and N_0 the number of central points. It should be noted that increasing the amount of central point experiments assists in evaluating the experimental error.

Another benefit of BBD is the ability to eschew extreme experimental conditions. If the corner (classical factorial) points constitute a hazard for the operator or are simply too harsh (causing a fault of the experimental set-up or any other potential for loss of data), employing BBD is a viable alternative for response surface mapping.

2.4. Taguchi Orthogonal Arrays DoE

Taguchi Orthogonal Arrays are designs that are, similarly to CCD, based around the factorial designs (full and/or fractional). However, instead of adding new points into the design matrix, Taguchi's approach favours an overlay of 2 traditional factorial designs (also referred to as the inner array and the outer array). For instance, Taguchi's 2^5 array can be viewed as a ¼ fraction of the full factorial design, resulting in 8 experiments instead of 32, positioned in a particular way as is depicted in Fig. 4 .

In Fig. 4 the red squares represent the factorial points (previously shown as red circles in Fig. 1 and Fig. 2), whereas the blue circles overlaying them are the design points of the outer array. The differences between such designs and classical factorial DoE matrices are subtle (as opposed to the major alterations needed for CCD). Taguchi-style frameworks distinguish between control variables and noise variables, placing the former into the inner array and the latter into the outer portion of the design space (Davis and John, 2018), thus allowing more control over the noise, which in turn, provides the operator with the ability to develop a robust process that could withstand alterations to the surroundings (which could be the ambient temperature or humidity if referring to agricultural crops; for ACs it could be positioning of the crucible in the furnace, precursor material variation or other lurking variables) without much influence on the control variable. Additionally, such designs allow for identification of interactions between the parameters, whilst maintaining the ability to evaluate the input factors separately (i.e. independent from one another) due to their inherent orthogonal nature. These designs can then be analysed using myriad statistical analysis techniques.

The basic and relatively small orthogonal arrays (L^8, L^9, L^{16} among others) can also be simply visualised *via* linear graphs (Fig. 5). However, the list of potential options for an experimental campaign is vast and includes myriad of available Taguchi designs.

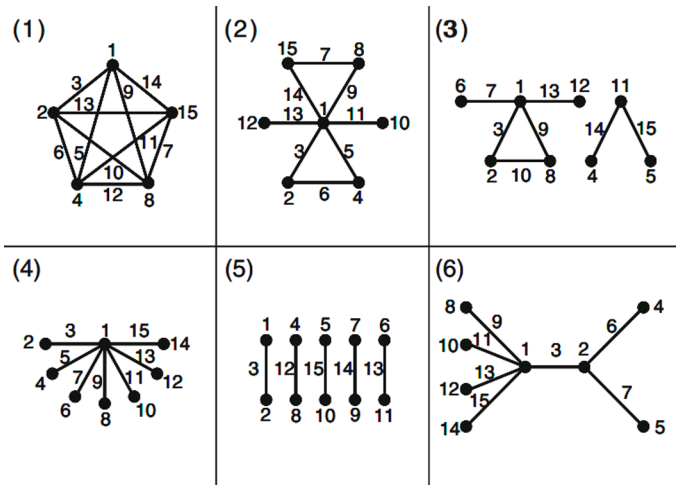

Fig. 5. – Linear graphs representing the L^{16} Taguchi orthogonal arrays (Suzuki et al., 2012).

Another great benefit of Taguchi designs is the ability to incorporate parameters at different levels without a sharp rise in the number of required experiments.

As a result, the choice of design is dictated by the objectives of the study and the stage at which the investigation is. Placket-Burman designs could be used for initial identification of fundamental features of the system, hence, preliminary screening. Full factorial techniques create a suitable experimental campaign providing coherent understanding of the design space as well as a "bird's-eye view" of the evaluated phenomenon as opposed to OFAT or Placket-Burman. Fractional factorial designs help to minimise the required number of experiments of a full factorial campaign, whilst still evaluating the design space and understanding the impacts of the studied factors. The main effects, however, can be contaminated by interactions. Some Taguchi designs, however, can evaluate a limited number of two-way interactions. Taguchi orthogonal arrays can be viewed as an alternative pathway to classical factorial designs, which are most appropriate when dealing with "outside" or uncontrollable parameters. They allow to create a process that is robust towards noise and lurking variables. Taguchi DoEs could also be used as a great tool for main effects estimation or screening, especially if the parameters are evaluated under different levels (i.e. mixed-level designs). CCDs could be employed as a build-up on a conducted factorial design to evaluate the non-linear nature of two-way interactions as well as to increase the design space (both due to presence of star (and central) points). They are a useful technique for response surface mapping as well as process optimisation. BBDs have similar objectives to CCDs but may result in a lower number of required experiments, hence, appropriate utilisation of resources. Further, they are preferable if evaluation of the extreme conditions (i.e. corner points) is not feasible.

2.5. Statistical Analysis Techniques

The most prominent analysis techniques featuring in this review are Analysis of Variance (ANOVA) and Response Surface Methodology (RSM). Fig. 6

ANOVA is a method to evaluate and separate any variation associated with the main effects within the experimental design, where the independent variables are discrete with three or more levels (Montgomery, 2017). It applies a least squares method to determine sources of variation within a dataset. In order to apply ANOVA, the following

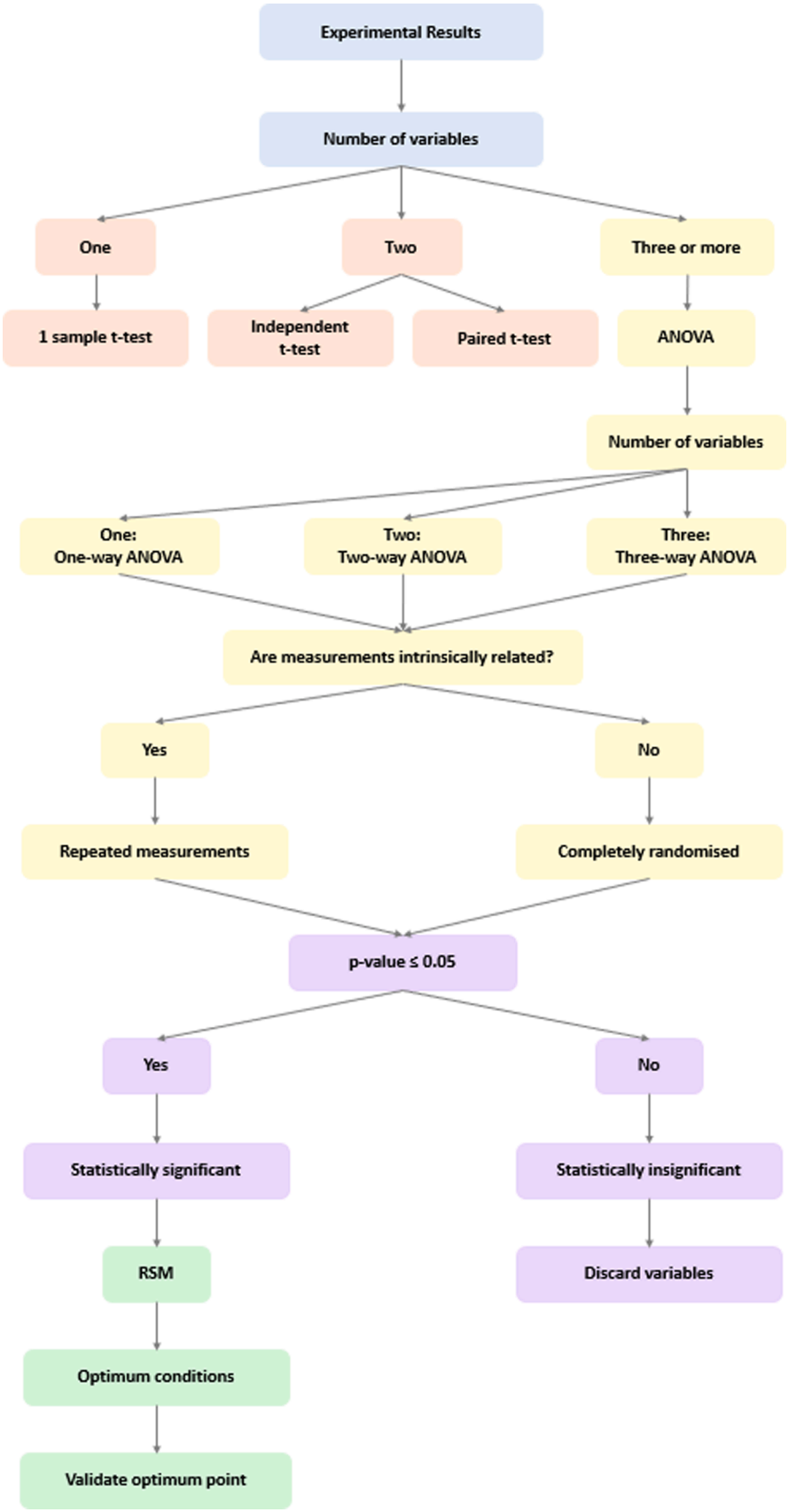

Fig. 6. – A simplified algorithm for statistical analysis.

assumptions must be fulfilled: every replicate must be independent of all others, and the experimental measurements must be completely randomised.

Prior to applying ANOVA, a normality test should be used to determine whether the data set is well modelled by a normal distribution (common normality tests include: Kolmogorov-Smirnov test, Lilliefors corrected K-S test, Shapiro-Wilk test, Anderson-Darling test, Cramer-von Mises test, D'Agostino skewness test, Anscombe-Glynn kurtosis test, D'Agostino-Pearson omnibus test, and the Jarque-Bera test) (Ghasemi and Zahediasl, 2012). Additionally, normality can be assessed visually using frequency distributions, stem-and-leaf plots, boxplots, P-P plots, and Q-Q plots; however, these techniques are usually considered to be less reliable (Ghasemi and Zahediasl, 2012).

Nevertheless, ANOVA is a popular method as it allows one or more factors, each at several levels to be tested simultaneously as well as assist in decision making, due to determination of statistical significance (represented as percent of contribution). Additionally, fewer replicates are required to make pairwise group comparisons when comparing ANOVA to other statistical techniques such as a student t-test.

Fisher (F) values determine the variance of a term with the variance of residual (Rashidi and Yusup, 2015) (variation between or within the samples in a data set). The larger the F-value, the higher the variation between sample means, relative to the variation within the samples.

The confidence level of ANOVA is confirmed by the probability value (p-value), which is a measure of probability that any observed difference could have occurred by random chance. It could also be viewed as the probability of achieving results close to the actual/representative of the experimental data (Rashidi and Yusup, 2019). The probabilities of the standard normal distribution, Z, could also be calculated using p-value tables (Pledger, 2008). When the p-value is sufficiently small (*i.e.* $\leq$ 0.05), it can be concluded with 95% confidence that there is a statistical significance between group means, and therefore, the null hypothesis can be rejected - The higher the F-value, the lower the corresponding p-value.

RSM is a useful tool in optimisation that can be used to visualise the effects various parameters may have on the response as well as to identify the frail points within the design space. However, applying ANOVA prior to RSM is beneficial because 3D plots only need to be produced if the combined effects are significant, thus, eliminating any insignificant terms.

RSM is applied to establish an empirical statistical model to develop an approximate relationship between a set of control variables (x_i) and a response variable (y) (Khuri and Mukhopadhyay, 2015), though, each factor has to be measured on at least three levels in order to generate either a 3D model or a 2D contour plot (in general 3D plots are preferred as a clearer picture of the response is observed). The relationship between the control (*i.e.* independent) variables and the response variable can be written as:

$$y = f(x_1, x_2, x_3 \ldots x_i) + \varepsilon \tag{5}$$

where the form of the true response function f is unknown, and ε is a term that represents other sources of variability not accounted for in f (such as measurement error, background noise etc.). The true response must be approximated using a low-order polynomial, such as first- or second-degree polynomial models. When applying the first-order model to two independent variables, the coded variables are as follows:

$$\eta = \beta_0 + \beta_1 x_1 + \beta_2 x_2 \tag{6}$$

The first-order model should be applied when approximating the true response within a relatively small area of the experimental region, where there is little curvature in f (Khuri and Mukhopadhyay, 2015).

The second-order model is more widely applied due to its flexibility and ability to use a variety of functional forms. Additionally, the parameters can be easily estimated using the method of least squares. The second-order model is coded as:

$$\eta = \beta_0 + \sum_{j=1}^{k} \beta_j x_j + \sum_{j=1}^{k} \beta_{jj} x_j^2 + \sum \sum_{i<j=2}^{k} \beta_{ij} x_i x_j \tag{7}$$

The model is then fitted to a data set generated by observing the response variable when the parameters are varied within the experimental region. RSM is useful to determine the optimum conditions and the significance of the factors and understand the nature of the relationship between them. Additionally, it can be used to predict the response at locations within the experimental regions (Khuri and Mukhopadhyay, 2015). RSM graphs can also be overlaid to compare and optimise several response variables simultaneously.

Less commonly used techniques include Pareto charts and perturbation plots (Dos Reis et al., 2016). Pareto charts highlight the most significant factors and interaction effects by displaying the absolute values of the effects. This is achieved by drawing a reference line on the chart, hence, when a factor exceeds the line, the effect is potentially important. The method employs an algorithm for producing statistically based acceptance limits (similar to confidence levels). Additionally, it is beneficial to critically evaluate the outcomes of a Pareto chart against a Normal Probability Plot (NPP). NPPs are produced by plotting the interaction effects of the parameters against the cumulative probability (%) (Antony, 2014). A straight-line graph should be produced for this method, any factors that deviate from the line are classed as an "active effect" or statistically significant. Perturbation plots are produced by varying one factor within a defined range while keeping all other factors constant. The plots allow researchers to compare the effects of all the factors at a particular point in the design space. Other analytical techniques that may also be utilised include: main effects plots, interactions plots and cube plots (Antony, 2014).

Post-experimental analysis is vital to ensure that valid conclusions can be derived from the data. The analysis phase can determine parameters that: yield the optimum performance, influence performance variability or affect the mean process performance. The majority of statistical software (in alphabetical order: Design-Expert, JMP, Minitab, SPSS, and etc) can assist in both analysis and creation of the desired DoE campaigns.

3. Optimisation of Adsorbents' Syntheses

3.1. Optimisation of Adsorbents' Porosity and Morphology via Variation of Synthesis Conditions

This section is dedicated to reviewing the works that have set out to optimise the morphological properties (namely, BET surface area (S_{BET}), micropore volume, micropore ratio and others) of various carbonaceous adsorbents using DoE techniques; outlining the synthesis conditions as well as identifying the most impactful parameters, describing the interactions between these parameters and briefly discussing the underlying reasoning. The discussed response variables are often employed as a proxy for evaluation of adsorption capacity. Such an approach, however, suffers from the great diversity of separation processes with many of them being influenced by myriad other factors (diffusion limitations, surface functional groups, activity and availability of active adsorption sites) apart from the produced porous structure. Nevertheless, the morphological properties can serve as a strong indication of the success of the thermal treatment as well as the nature of the produced adsorbent.

3.1.1. Factorial DoE

Exactly the same experimental matrix as shown in Fig. 1a has been applied to investigate synthesis of activated carbon (AC) from olive cake waste by means of chemical activation with KOH (Abdel-Ghani et al., 2016). The factors and the levels were chosen in accordance with preliminary experiments and identified as activation temperature (T_{act}) of 600 and 900°C (X_1), holding/activation time (τ_{act}) of 1 and 3 h (X_2), and impregnation ratio (IR) of precursor to activation agent of 1:2 and 1:4

(X_3) utilising a 2^3 full factorial DoE using Minitab software. It should be noted, however, that when evaluating parameters at only 2 levels, identification of non-linear relationships (*i.e.* curvature) is impossible, leading potentially to false conclusions. All process variables were found to have a significant impact ($p<0.05$) on the BET surface area with the τ_{act} being the most impactful parameter followed by the three-way interactions and then T_{act}. The authors identified the optimum preparation conditions to be at the lowest levels of the investigated factors for such chemical activation. However, other activation agents and routes as well as precursor materials will yield different optimum points. For instance, (Dos Reis et al., 2016) has investigated the effects of changes in input variables for both conventional and microwave pyrolysis of sewage sludge with $ZnCl_2$ as activating agent. The studied factors for the conventional activation process were τ_{act} (X_1^1, 15 – 60 min), T_{act} (X_2^1, 500 – 800°C) and agent/sludge ratio (X_3^1, 0.5 – 1.5), while the preparation conditions for the microwave methods varied greatly. The hold time was significantly smaller (X_1^2, 8 – 12 min) and the activation temperature was substituted by the supplied power (X_2^2, 700 – 980 W); however, the IR was kept the same for both of the AC synthesis routes. The BET surface area was maximised under the following conditions: furnace – 500°C for 15 min, microwave– 980 W for 12 min, while maintaining an IR of 0.5 for both activation pathways. It is noteworthy that for the conventional method, T_{act} was the most significant factor affecting the S_{BET} (for microwave – the interaction between ratio and power) and the second was the three-way interaction. In contrast, the second most important factor for microwave activation was the holding time, which was found to be positive. If comparing the two activation routes, the authors have demonstrated the specific volume of pores, the micropore surface area and S_{BET} to be larger for the conventional method than for the microwave activation (with a higher bulk density for the latter). These differences were attributed to the impact of radiation on the decomposition kinetics of the organic compounds. Microwave energy is transformed into heat by dipole rotation and ionic conduction. Such quick volumetric heating promotes development of pores over a shorter time span, hence, saving energy.

Fractional factorial designs have also been implemented in the literature (Bergna et al., 2020) to investigate the effects of several process variables on a number of outputs for AC production *via* physical activation of peat with steam using MODDE 9.1 by Umetrics software. Within the chosen framework, the reactor (rotating quartz tube in an oven) rotation speed (X_1, 4.36 – 17.44 rpm), initial turf mass (X_2, 100 – 300 g), heating rate (X_3, 2.6 – 13°C/min), inert gas flow rate (X_4, 100 – 300 ml/min of N_2), oven temperature (X_5, 700 – 800°C), τ_{act} (X_6, 1 – 4 h) and steam flow rate (X_7, 30 – 120 g/h) were adjusted. Despite evaluating 7 factors at 2 levels each, and conducting 3 repetitions at the central point, a matrix of only 19 runs has sufficed, thus, highlighting the value of DoE. With regards to the overall activation process τ_{act}, T_{act} and steam feed were identified as the most influential parameters, strongly affecting the yield and total carbon content of the final product, but aiding the development of micro and mesoporosity, hence, the BET surface area. Rotation speed, the fourth most influential (and often discarded parameter for AC production) factor of the study, had a negative effect on the adsorption characteristics of the AC with a notable exception of benefiting the formation of mesopores (likely due to better contact of the steam with the biomass), though to a much lesser extent than the 3 key identified variables. The authors have also identified the initial mass of the sample to have little to no impact on the outputs, since porosity creation *via* carbon-steam reaction rate is governed by the gas-surface interaction rather than gas-mass (Kiel et al., 1975). However, the authors acknowledged that the miniscule yield gradient (1.4%) might be associated with the quite narrow range of the investigated levels of X_2 and as such an increase of the initial mass may more vividly affect the outcome when scaling up the process.

3.1.2. Central Composite DoE

Such a route has been previously taken in the literature

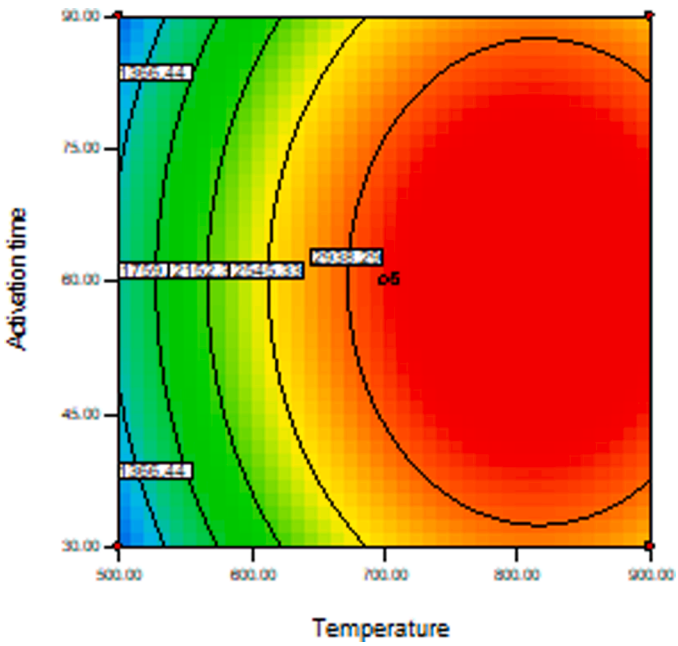

Fig. 7. – A contour plot for specific surface area as a function of activation time and temperature (Gao et al., 2015).

(Loredo-Cancino et al., 2013) upon discovering an imminent inflection point within the explored range of variables during optimisation of AC synthesis from barley husk. The independent variables were the IR (X_1, 0.5 – 1.5 g $ZnCl_2$/g precursor) combined with the τ_{act} (X_2, 20 – 180 min) and T_{act} (X_3, 300 – 700°C), while the desired responses were maximum iodine number (a proxy for estimating surface area) and AC yield. Utilising Design-Expert software, ANOVA, RSM and a dual optimisation approach by quadratic models, the authors have determined the optimum preparation conditions for improving both of the responses simultaneously to be at 1.1 mass ratio, 20 min and 436°C. However, the optimum points for each individual Y varied greatly between one another. Thus, to arrive at a point of simultaneous optimisation of both control variables, a desirability function was deployed (described at length in section 4.1.2). Both of the outcomes were considered to be of equal value, hence, assigning the same weight of one to both yield and iodine number.

Moreover, (Rio et al., 2005) performed an intelligent DoE with CCD to optimise synthesis of carbonaceous sorbents from sewage sludge. Although, their design and results are discussed at length in section 3.2.1 of this review, it is noteworthy, that the authors have shown T_{act} to affect the S_{BET} and micropore volume, whilst changes in τ_{act} and IR have been demonstrated to be positive. Furthermore, these three parameters have also had a positive impact on mesopore development within the investigated levels. Additionally, in their investigation the trials have been randomised in order to reduce errors from the possible lurking variables. Such diminishment of the uncontrollable effects (often referred to as the lurking variables) is desired when employing DoE matrices.

3.1.3. Box-Behnken DoE

(Gao et al., 2015) have employed this DoE framework to evaluate the preparation method of an AC from a green alga for use as an electrode material. In their investigation a total of 17 samples were synthesised (since here $P = 3$, leading to 12 factorial points, and $N_0 = 5$, meaning 5 repetitions in the central position) to study the influence of altering T_{act} (X_1, 500 – 900°C) and τ_{act} (X_2, 30 – 90 min) together with the activating agent/char ratio (X_3, 0.5 – 3.5) on the BET surface area and micropore ratio as well as mean pore size of the final product (if the authors were to employ a CCD for the same set of process variables, the experimental campaign would have comprised of 20 experimental runs containing 8

factorial, 6 axial and 6 central replications). The data has been analysed using Design-Expert 7.0 software and RSM technique. The responses suggest the optimum preparation conditions to be 850°C for an hour with an IR of 1.1 (KOH to precursor) with the T_{act} being the most significant influencing factor on surface area (F-value = 129.35), whilst the interactions between the parameters were found to be effectively insignificant due to the circular nature of the contour plots as can be seen in Fig. 7 .

T_{act} was also found to possess a pronounced effect on the micropore ratio (F-value = 47.43) and the mean pore size (F-value = 130.54), though the interaction between the temperature and IR also contributed significantly to the changes in both outputs (15.36 and 121.20, respectively), thus, depicting the intensification of the synthesis conditions to propagate widening of micropores, hence, the transition towards meso and macropores.

3.1.4. Taguchi Orthogonal Arrays DoE

Most of the experimental design frameworks described in Taguchi's catalogue are mixed level designs (Kacker et al., 1991) and these designs have been widely deployed when evaluating adsorbent synthesis. For instance, (Loloei et al., 2017) have used a mixed level L^{16} (2^2 x 4^4) Taguchi orthogonal array for the means of AC production optimisation *via* a two-step activation process. The investigated factors with 4 levels were pyrolysis/carbonisation temperature (X_1, 550 – 700°C) and holding time (X_2, 30 – 120 min) as well as T_{act} (X_3, 800 – 950°C) and τ_{act} (X_4, 30 – 120 min) while the heating rate and CO_2 flow rate were only changed from 5 to 10°C/min and from 400 to 600 ml/min, respectively. Their optimised synthesis route for maximising the iodine number was stated to be at carbonisation temperature and time of 700°C for 60 min, T_{act} and τ_{act} of 900°C for 60 min and at a CO_2 flow rate of 400 ml/min. To maximise the yield, the process conditions should be kept largely the same, with the only difference being τ_{act} and T_{act} should be maintained at the lowest studied levels. These findings are in good agreement with the literature as longer time and temperature of the activation process promote surface pore development leading to a diminishment of the final product yield but also to a possible increase in adsorption properties. Therefore, the T_{act} and τ_{act} have been stated to be the key variables (respectively), possessing the highest F-ratios and having the biggest influence on the properties of the AC. It is noteworthy, that the optimised conditions described for the different responses do not feature the heating rate. This was attributed to the minute differences in final product properties when elevating the ramp rate from 5 to 10°C/min. In their further works (Loloie et al., 2017) the authors have compared the responses for the iodine number with the responses for the specific surface area (SSA). The results suggest that these outputs are analogous in nature as the optimum sample in their later study was produced at the exact same conditions bar the exception of the temperature of the first pyrolysis step where maintaining the AC precursor at 650°C facilitated the highest BET surface area. Similarly, the most influential parameter was T_{act}.

The Taguchi orthogonal arrays have also been utilised to optimise activated carbon fibre (ACF) production out of waste cotton (Ekrami et al., 2014). The chemical activation procedure conditions, *i.e.* τ_{act} (X_1, 0.5 – 3 h) and T_{act} (X_2, 350 – 500°C), IR (X_3, H_3PO_4/precursor mass = 0.5 – 3) and heating rate (X_4, 2 – 20°C/min), were varied to identify their impacts on product yield and iodine number. The optimum conditions to compromise between the antagonistic effects of the formerly-mentioned process variables were identified at 450°C for half an hour at a ramping rate of 10°C/min while doubling the agent-to-precursor mass ratio. Interestingly, the obtained p-values for all of the parameters were greater than 0.05 with regards to the iodine adsorption, though, the temperature of activation had the highest F-value followed by the IR. In the case of ACF yield, T_{act} and τ_{act} were found to be significant with the former possessing a higher F-value and a lower p-value.

3.2. Optimisation of Adsorbents' Capacity via Variation of Synthesis Conditions: Gaseous Media

This section (*as well as section 3.3*) endeavours to discuss and review published research on the topic of optimisation of the carbonaceous sorbent's capacity (i.e. uptake) for a given adsorbate in gaseous (*aqueous for section 3.3*) media. As with the previous section the experimental matrix as well as the influence and significance of various synthesis conditions and (their interactions) is outlined.

3.2.1. Central Composite DoE

A central composite design created *via* Design-Expert 8.0.5 software containing 20 experiments (including the ANOVA and RSM studies) was employed to investigate the impact of activating agent IR (X_1, H_3PO_4 to AC precursor = 0.66 – 2.34), τ_{act} (X_2, 69.55 – 170.45 min) and T_{act} (X_3, 381.82 – 718.18°C) on a number of output parameters such as yield, iodine number and CO_2 adsorption capacity (Khalili et al., 2015). The latter was shown to be influenced by all of the formerly mentioned input variables and their interactions (p-values < 0.05), though the IR had the greatest antagonistic effect showing the highest F-value. The other two responses were found to be strongly impacted by the variations in τ_{act} (showing the lowest p-values and maximum F-ratios). The authors have also optimised the AC preparation procedure in order to compromise between the dependent variables utilising a desirability function (this technique is described at length in section 4.1.2). The sample achieving high micropore volume and surface area whilst maintaining a respectable product yield was prepared by impregnating the precursor with H_3PO_4 with an agent ratio of 2.2 and activating for 170.45 minutes under 488.82°C. The increase in τ_{act} and T_{act} led to enhanced CO_2 adsorption. This phenomenon might be associated with formation of micropores which positively impact this response variables. These micropores could be formed due to the release of tarry matter or disorganised carbon that was blocking the pores. Alternatively, formation of micropores could be attributed to a larger amount of phosphorus being incorporated into the precursor when elevating X_2 and X_3 in the form of phosphates or polyphosphates. Hence, their removal might be "at fault" for the formation of micropores. However, increasing the IR led to a drop in uptake. The antagonistic impact is perceived to be the result of micropore destruction, which affects the CO_2 adsorption capacity of the AC.

CCD has also been used to evaluate the impact of time (X_1, 20 – 220 min), temperature (X_2, 532 – 868°C) and H_2SO_4 (X_3, 0.15 – 1.85) IR on the production of carbonaceous adsorbents from sewage sludge (Rio et al., 2005). The authors have analysed 13 different material properties (employing STATGRAPHICS® software) as their targeted responses. Such a vast number of desired outcomes has made optimisation inherently difficult due to the contradictory nature of some of the dependent variables. Therefore, the authors have denoted two different sets of optimised activation conditions in order to find a compromise between the various outputs. The procedure for developing optimal micropore volume as well as maximising both acetone and toluene adsorption capacities simultaneously whilst adhering to their targeted 35 – 40% final product mass yield was found to be at τ_{act} and temperature of 145 min and 700°C with the IR of sulfuric acid to sewage sludge of 1.5:1. The authors concluded that all effects and interactions were of significance (especially the quadratic effect of T_{act} leading to an extremum point at 700°C, thus, proving the applicability and necessity of a CCD design for the experimental campaign) and summarised the impact of IR and τ_{act} to be positive, whilst emphasising the T_{act} to affect the volatile organic compounds (VOCs) sorptive properties.

3.2.2. Box-Behnken DoE

(Yu et al., 2020) investigated the possibilities of synthesising activated carbon as an adsorbent for CO_2 capture. In their study, the Box-Behnken design was employed to evaluate the effect of 3 parameters (mass ratio of activating agent to carbon precursor, X_1; τ_{act}, X_2; T_{act}, X_3)

at 3 different levels (1:0.5 – 2.5; 0.5 – 2 hours and 650 – 850°C, respectively). In order to obtain the optimum adsorption capacity as well as the yield of final product, the authors developed an experimental campaign consisting of 17 runs with 5 repeating experiments on the central point to validate their model. Design-Expert software has been used to determine the number of trials. In addition, ANOVA was applied to determine the significant contributors to each of the response variables separately. Their findings propose that boosting the T_{act} leads to a diminishing AC yield, due to the degree of polycondensation reactions. They have also observed an apparent trend of growing significance of the interaction between τ_{act} and T_{act} as the latter rises. This phenomenon was explained by strengthening of the reaction between the activating agent (KOH) and the coal tar pitch used as carbon precursor as the T_{act} maximizes, therefore, leading to a lesser yield of the final product. Furthermore, pore creation and pore widening determine the adsorption capacity of the material. In fact, as ultramicropores (< 0.7 nm) are most suitable for immobilising carbon dioxide molecules, finding the optimum point for these competing processes is of utter importance. It is suggested that long τ_{act} vastly affects pore creation, shifting the equilibrium towards pore widening. This effect is pronounced stronger at higher temperatures, *i.e.* relatively low temperatures favour creation rather than widening of pores. Therefore, the optimum capture capacity was found to be at the following preparation conditions: 650°C for 1.25 hours with the KOH IR of 2.5: 1. Others (Rashidi and Yusup, 2019) have also used BBD to optimise AC production for carbon capture, although *via* a single-step physical activation. In this study, the independent variables were selected to be inert gas flow rate (X_1, 150 – 450 ml/min) together with τ_{act} (X_2, 60 – 120 min) and T_{act} (X_3, 750 – 950°C). As thermal activation techniques lack an activating agent, the most determining factor was learned to be T_{act}. This parameter possessed the greatest F-value and a p-value smaller than 0.05. The optimum activated carbon sample was activated at 850°C under the maximum flow rate and minimum time out of the investigated levels. It is noteworthy, that these conditions have been chosen on the basis of the maximum adsorption capacity, rather than as a function of both capacity and product yield. The reasoning behind this decision was that these experimental conditions provide an adequate final product yield (exceeding the minimum industrial target provided in the literature). Nevertheless, when evaluating more than one output parameter, it is favourable to apply a function of desirability in order to maximise all of the targeted responses simultaneously. The authors did, however, randomise the sequence of their trials which, as mentioned previously in the review, is a favourable practice when conducting an intellectually designed experimental campaign.

3.2.3. Taguchi Orthogonal Arrays DoE

A large orthogonal array consisting of 25 experiments (L^{25}) has been employed within the Taguchi experimental design framework by (Rashidi et al., 2013) to evaluate the Signal-to-Noise (S/N) ratios for 6 varying factors such as: precursor (X_1, Coconut fibre, coconut shell, palm kernel shell, palm mesocarp fibre and rice husk), particle size (X_2, 250 – 1000 μm), heating rate (X_3, 5 – 25°C/min), flow rate (X_4, 100 – 300 ml/min), T_{act} (X_5, 500 – 900°C) and τ_{act} (X_6, 15 – 90 min). Each parameter has been evaluated at 5 different levels within the boundaries outlined above. The key factor influencing the gas sorption capacity was determined to be the T_{act} due to the activation process being endothermic. However, the composition of the original material has also been noted to play a crucial role as it has the highest impact on the ash and carbon contents of the final adsorbent. The authors have elaborated on this in their further work (Rashidi and Yusup, 2015) performing ANOVA and outlining the p-values (and F-values) for the formerly mentioned parameters to be > 0.0001 (23.10) and 0.0074 (5.88), respectively. This analysis has been performed utilising Design Expert® version 8.0 software. The optimum sample has been identified to be produced from 250 μm coconut shell particles that were activated at 900°C for 45 min under a CO_2 flow of 150 ml/min and a ramping rate of 20°C/min. When evaluating carbonaceous adsorbent precursors, understanding the carbon content of each of the materials is imperative. Since for physisorption the carbon surface immobilises the adsorbate *via* weak van der Waals forces, a larger quantity of C would imply potentially higher adsorption capacity. On the other hand, the amount of ash in the precursor also plays a crucial role as these particles may block the pores, hinder porosity development and, hence, uptake.

3.3. Optimisation of Adsorbents' Capacity via Variation of Synthesis Conditions: Aqueous Media

3.3.1. Factorial DoE

Full factorial design has been commonly applied to optimise the synthesis of activated carbon (Alam et al., 2009), (Lim et al., 2020). For instance, (Alam et al., 2009) optimised the synthesis of powdered activated carbon from oil palm empty fruit bunches. The method applied a 2-level full factorial design with two central points and a total of 10 experiments, developed on the Design Expert software (version 6.0.8). The effects of three experimental factors were investigated; T_{act} (X_1, 600 – 900°C), τ_{act} (X_2, 15 – 45 min) and CO_2 flow rate (X_3, 100 – 250 ml/min) to optimise the adsorption capacity and yield, whereas ANOVA and RSM were applied to determine the significance of the factors and the optimum conditions. The optimum conditions were T_{act} of 900°C, τ_{act} of 15 min and a CO_2 gas flow rate of 0.1 L/min. Temperature was found to be the most significant factor for both adsorption capacity ($f = 521.67$, $p = 0.001$) and yield ($f = 1936.85$, $p = 0.0005$). Adsorption capacity increased with increasing T_{act} and decreasing τ_{act} and CO_2 flow rate. The highest carbon yield was obtained when all of the variables were at the minimum value. Elevated temperatures increase the burn-off of carbon, causing the pores present within the structure to become more developed and the pore volume to increase. Additionally, any volatile materials and tar blocking the pores are removed, optimising the adsorption capacity. However, increased burn off causes a decrease in yield, thus, leading to a trade-off between yield and adsorption capacity when selecting the optimum conditions. The R^2 values for the models were calculated to be 0.9964 and 0.9992 for adsorption capacity and yield, respectively. Both models had R^2 values close to unity and standard deviations of ≤ 0.2, indicating that the theoretical values correlate with their experimental counterparts.

3.3.2. Central Composite DoE

CCD has been widely implemented to evaluate the synthesis conditions of carbonaceous adsorbent for pollutants removal from aqueous media (Hoseinzadeh Hesas et al., 2013, Garba et al., 2014, Mozaffarian et al., 2019, Tan et al., 2008, Basheer et al., 2019). For example, an AC has been synthesised from waste palm shell using microwave radiation and zinc chloride as the activation agent (Hoseinzadeh Hesas et al., 2013). CCD was applied to optimise yield and methylene blue (MB) adsorption capacity by investigating four factors on three levels, namely τ_{act} (X_1, 10 – 20 min), microwave power (X_2, 900 – 1200 W), IR (X_3, 1.13 – 2.25) and particle size (X_4, 1 – 2 mm). The experimental design consisted of 16 factorial points, 8 axial points and 6 replicates at the centre points, for a total of 30 experiments. However, CCD is usually only applied for three or less factors since an excessively increased number of (steady-state) experimental runs may lead to the introduction of errors into the experiment. When working with four or more factors, it is advisable to split the matrix into blocks of relatively homogeneous experimental conditions, allowing for independent estimates of the block effects (Antony, 2003). Effects of variation due to noise factors would be eliminated, hence, improving the efficiency of the experimental design. 3D response surface plots were analysed using Design Expert software (version 7.1.5) to determine the optimum conditions. Yield and adsorption capacity were maximised at τ_{act} of 15 min, a microwave power of 1200 W, a $ZnCl_2$ impregnation ratio of 1.65 and a particle size of 2 mm. The significance of the factors was determined using ANOVA. τ_{act}, microwave power and IR had a significant effect on

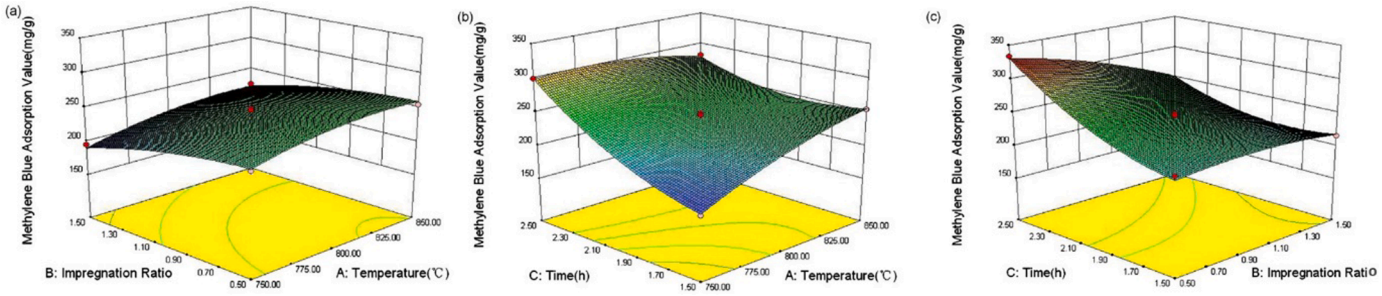

Fig. 8. – 3D response surface plots for combined effects on the MB adsorption value: (a) IR and temperature, t = 2 h; (b) time and temperature, IR = 1.0; (c) time and IR, T = 800 °C (Chen et al., 2013).

AC yield, while all 4 factors were significant for MB adsorption. Among them, T_{act} had the most significant effect on yield ($f = 265.14$, $p < 0.0001$) microwave power impacted MB adsorption the most ($f = 62.07$, $p < 0.0001$). Additionally, all interactions were found to be statistically significant for both of the responses. $X_2\ X_4$ had the greatest impact on yield ($f = 27.88$, $p < 0.0001$), whereas MB adsorption was the most sensitive to $X_1\ X_3$ ($f = 41.80$, $p < 0.0001$). The factors were further investigated using 3D response surface plots. At lower τ_{act}, yield was not significantly affected by increases in microwave power and IR, this was attributed to lack of time for the reaction to take place between the activation agent and carbon. However, as τ_{act} was increased, microwave power had a larger effect on yield, credited to increased burn off and pore widening. MB adsorption was maximised when both τ_{act} and microwave power were at the highest value due to the development of the porous structure and increase in available active sites. No considerable changes were observed when increasing IR due to excess chemical agent blocking the pores and available active sites. The predicted carbon yield and adsorption capacity were 65.484% and 96.93%, respectively. Experimental values were both slightly lower at 64% and 95.95%. The model was determined to be of sufficient accuracy due to the low relative errors of 2.26% for yield, and 1.01% for adsorption capacity.

Garba *et al.* applied CCD to optimise the preparation of AC from *Borasus aethiopum* (a type of palm) shells *via* chemical activation (Garba et al., 2014). The experiment consisted of eight factorial points, six axial points and six replicates giving a total of 20 experiments. Three factors were investigated; IR (X_1, 1.17 – 4.03), T_{act} (X_2, *571* – 779°C) and τ_{act} (X_3, 0.79 – 2.81 h). Design Expert software (version 6.0.6) was employed to determine the optimum activation conditions, which were as follows: T_{act} and τ_{act} of 713°C and 2 h 49 min, respectively and an IR of 1.33. ANOVA was applied to investigate the significance of the factors. The model indicated that τ_{act} to be the most significant factor ($f = 94.83$, $p < 0.0001$). The mechanism for chemical activation using hydroxides has been proposed previously, for example (Lillo-Ródenas et al., 2003). hypothesised that the reaction between NaOH and carbon is as follows:

$$4NaOH + C \rightleftharpoons 4Na + CO_2 + 2H_2O \quad (8)$$

According to equation 1, an increased τ_{act} prolongs the reaction time between NaOH and carbon, therefore, removing any disordered carbon in the form of CO_2. Physical activation will also take place as more CO_2 is generated throughout the reaction, increasing the porosity and adsorption capacity but decreasing the yield. Nevertheless, $X_2\ X_3$ interactions between had the most significant combined effect ($f = 14.88$, $p = 0.0019$). Additionally, the 3D plots indicated that increasing both IR and temperature would affect the AC yield, though, no notable effects were observed when increasing τ_{act}.

3.3.3. Box-Behnken DoE

Many studies have applied BBD matrix, when evaluating 3-factors at 3-levels. This method consists of a total of 15 experiments, involving 12 factorial runs and 3 replicates at the central point (Jung et al., 2019, Chen et al., 2013, Pereira Da Silva et al., 2019, Md-Desa et al., 2016), with commonly investigated factors including IR, T_{act} and τ_{act} to optimise response variables such as carbon yield and adsorption capacity. For instance, (Jung et al., 2019) used a BBD-based quadratic model to optimise the synthesis of AC/iron oxide magnetic composites using marine microalgae as the precursor. The effects of IR (X_1, 1:1 – 3:1), T_{act} (X_2, 600 – 800°C) and τ_{act} (X_3, 60 – 180 min) on the production yield and acetylsalicylic acid adsorption capacity were investigated. Design-Expert (version 6) and SAS (version 9) packages were applied to design and statistically assess the experiment. The optimum conditions were determined to be τ_{act} and T_{act} of 129.26 min and 727.09°C, respectively, and an IR of 2.62:1. The conditions achieved an overall yield and adsorption capacity of 60.44% and 69.09 mg/g, respectively. ANOVA was used to establish the most significant factors; it was found that T_{act} had the most significant impact on yield, and IR on adsorption capacity. RSM plots were created using the selected polynomial quadratic regression models. The plots indicated that all independent variables had a negative influence on the yield due to the removal of volatile matters and tar leading to a greater weight loss. The opposite trend was observed for adsorption capacity due to functionalisation of the surface and development of the porous structure.

BBD has been used to investigate the production of AC from kenaf core using $K_2C_2O_4$ as the chemical activation agent (Chen et al., 2013). The method sought to optimise iodine and MB adsorption by evaluating the effects of three factors, T_{act} (X_1, 750 – 850°C), IR (X_2, 0.5 – 1.5) and τ_{act} (X_3, 1.5 – 2.5 h). The BBD method was determined using Design Expert (Trial Version 7.0.0) software. The optimum conditions were as follows: T_{act} of 800°C, IR of 0.65 and τ_{act} of 2.5 h. Use of ANOVA determined that all the studied factors were significant. IR followed by τ_{act} and their interaction were identified as having the most significant impact on the iodine number. Whereas, τ_{act}, followed by IR and the combined effects of τ_{act} and T_{act} had the most significant impact on MB adsorption. RSM indicated that the optimum yield was achieved in a region where IR was at the minimum value and τ_{act} was at its maximum point. Whereas, decreasing T_{act} and increasing τ_{act} gave the optimum value for MB and I_2 adsorption capacity of 323.19 mg/g and 1185.17 mg/g, respectively (Fig. 8).

3.3.4. Taguchi Orthogonal Arrays DoE

(Liu et al., 2013) and (Makeswari and Santhi, 2013) employed the Taguchi design matrix, using an L_{16} orthogonal array with four operational parameters each on 4 levels, hence, 16 experiments in total. The former optimised the synthesis of activated carbon form *Spartina alterniflora* using chemical activation with the investigated parameters being carbonisation temperature (X_1, 400 – 550°C), KOH:char IR (X_2, 1:1 – 1:4 wt/wt), T_{act} (X_3, 600 – 850°C) and τ_{act} (X_4, 30 – 120 min). The study aimed to optimise the iodine number (iodine, mg/g carbon). In order to investigate the influence of the operational factors on iodine number, the ANOVA technique was employed to determine S/N ratios using SPSS (version 13.0). The optimum synthesis conditions for X_1, X_2, X_3, X_4 were found to be 450°C, 3:1, 90 min and 800°C, respectively. The factors were analysed by calculating the percentage contribution using the following

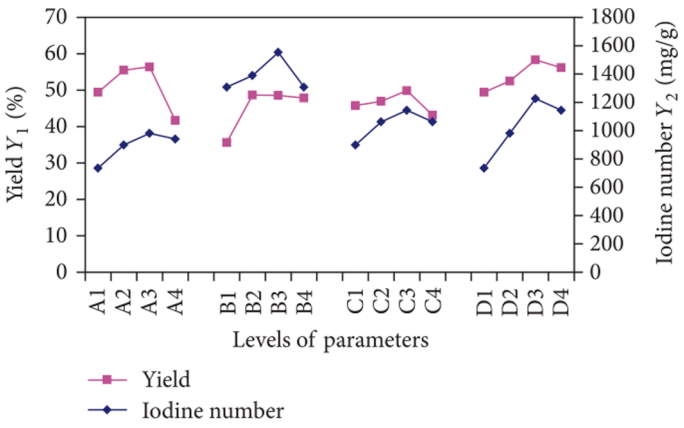

Fig. 9. – The effect of operational parameters on responses of the prepared samples, (A) radiation power, (B) radiation time, (C) concentration of $ZnCl_2$, and (D) impregnation time (Makeswari and Santhi, 2013).

equation:

$$\%\ contribution = \frac{Sum\ of\ Squares}{total\ Sum\ of\ Squares}\ x\ 100 \tag{9}$$

The analysis showed that T_{act} had the largest contribution (82.65%) on adsorption capacity. Increasing the temperature up to 800°C increased adsorption capacity; however, temperatures greater than 800°C had a negative impact. Similar trends were observed for impregnation ratio and τ_{act} when the conditions were above 3:1 and 90 minutes, respectively. This was attributed to the collapse of micropores, reducing surface area and adsorption capacity.

(Makeswari and Santhi, 2013) studied microwave-assisted chemical activation using zinc chloride to prepare activated carbon form *Ricinus communis*. The parameters investigated were microwave radiation power (X_1, 100 – 600 W), microwave radiation time (X_2, 4 – 10 min), concentration of $ZnCl_2$ (X_3, 30 – 60 vol%) and impregnation time (X_4, 16 – 28 h). The study aimed to maximise iodine number and yield. The optimum responses were determined by plotting the experimental yield and $ZnCl_2$ concentration to determine the optimum conditions for radiation power (100 W), radiation time (8 min), concentration of $ZnCl_2$ (30 %) and impregnation time (24 h). The study concluded that radiation time and concentration of $ZnCl_2$ were important factors for yield, whereas, iodine number was only significantly impacted by concentration of $ZnCl_2$. To identify the optimum conditions, the researcher produced a graph which included each level of each parameter along the x axis and the response factors along the y axis (Fig. 9); however, the study would have additionally benefited from applying ANOVA, because the results were not analysed statistically and therefore, it cannot be determined whether any of the factors are of significance to the response.

4. Optimisation of Adsorption Processes

The following portion of our review paper is dedicated to reviewing the application of the formerly-mentioned DoE frameworks for optimisation of the process of adsorption on the carbonaceous material (section 4.1 evaluates the sorption process of gas-phase adsorption, whereas section 4.2 is focused on aqueous media) as opposed to optimising the synthesis routes of the sorbent (section 0). Thus, this section covers the impact of adsorbate concertation and flow rate, the temperature and duration of the process and other parameters (e.g. pH of the system and etc.).

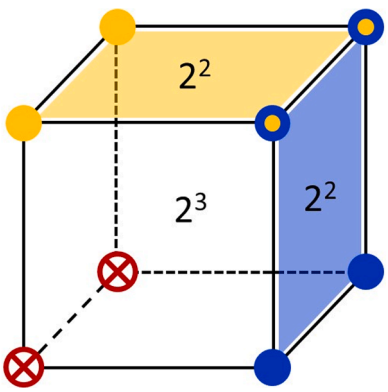

Fig. 10. – Comparison of the design space employing a single 2^3 design (cube in black) vs two overlapping 2^2 designs (yellow and blue). The crossed out red corners represent the originally proposed design points that were unfeasible.

4.1. Optimisation of Adsorbents' Capacity via Variation of Process Conditions; Gaseous Media

4.1.1. Factorial DoE

The full factorial experimental matrix has been employed widely in the literature (Hsi and Chen, 2012, Miller et al., 2000, Liu and Ritter, 1998). For instance, using a three-factor two-level design (2^3) design, (Muzic et al., 2010) investigated diesel fuel desulfurization. Desulfurization of the fuel was achieved *via* adsorption using commercial AC and 13X zeolite. The design investigated the effect of adsorbent mass (X_1, 2.00 and 4.00 g), adsorption temperature (T_{ads}, X_2, 30.0 and 70.0°C) and time (τ_{ads}, X_3, 20 and 100 mins) on the adsorbent capacity (q_i, mg/g) and residual sulphur content (C_i, mg/kg). It was found that the interactions between the studied factors were minimal in contrast to the effects of individual parameters, with adsorbent mass and τ_{ads} contributing the largest effect on C_i at 83.87% and 7.44% and on q_i at 91.12% and 3.17%, respectively. The multiple regression analysis in Design-Expert software determined a model describing the effects of the three factors on C_i and q_i accounting for over 94% of the variability.

(García et al., 2011) employed RSM to study the combined effect of the adsorption CO_2 partial pressure (P_{CO2}, X_1, 1 – 3 bar) within a total pressure of 5 to 15 bar and T_{ads} (X_2, 25 – 65°C) on CO_2 capture capacity and breakthrough time. The three-level two-factor full factorial experimental campaign consisted of 13 experiments (nine factorial points and four replicates at the centre of the design that make it possible to estimate any experimental error). CO_2 partial pressure was identified as the primary influencer on both capture capacity and t_b. Using ANOVA, statistical significance was evaluated, the two second-order models were statistically significant and their lack of fit found to be not significant (at a 95% CL). The Adj-R^2 and the absolute average deviation (AAD) values were acceptable at 0.969 and 3.4%, respectively for CO_2 capture capacity; and 0.984 and 2.0 respectively, for breakthrough time. Interestingly, no interaction effects between the two independent variables were found. Both capacity and t_b were found to be proportional to P_{CO2} and inversely to T_{ads} and the square of T_{ads}. Response plots elucidated to response curvature, indicating that the effect of temperature varies over the experimental range.

In the assessment of combined thermal and vacuum adsorption (VTSA) in the work of (Ramalingam et al., 2011) a factorial design of experiment was employed and validated *via* process simulation. The regeneration performance was evaluated by considering bed regeneration rate, concentration of recovered VOCs and operating costs. The VTSA process involved thermally regenerating the spent activated carbon with hot nitrogen followed by vacuum desorption. The factorial design considered the effect of the thermal regeneration operating parameters, with the vacuum desorption parameters remaining constant. Nitrogen gas temperature (T, X_1, 85 and 93°C), nitrogen flow rate (V_f,

X_2, 0.07 and 0.14 NL/h) and intermediate regeneration percentage (I_R, X_3, 55 and 75 %) were varied, and the recovery percent (*FR*) and operating costs (OP_{EUR}) measured. However, due to an inability to achieve $I_R = 75$ % at $V_f = 0.07$ NL/h, a 2^3 design had to be abandoned in favour of two 2^2 campaigns. The first 2^2 studied T and I_R whilst fixing V_f at 0.14 NL/h, the second 2^2 studied T and V_f whilst fixing I_R at 55%. Given that two (out of four) of the experiments defined in both designs evaluated the same desorption conditions, the total number of trials run was 6 and not 8 as to be expected from two 2^2 designs.

Although an ingenious solution to overcome equipment limitations, Fig. 10 illustrates the significant reduction in design space (effectively studying only two sides of the initially proposed domain). The authors could have benefitted from selecting levels for each factor that were attainable within the confinements of the experimental setup; quite clearly two 2^2 designs is not a comparable substitute for a 2^3 matrix. Alternatively, optimisation with BBD could be a promising avenue as it paves the way for designing a campaign "around" potential data-loss points. Regardless, selection of appropriate (attainable yet impactful) levels for the evaluated parameters facilitates production of reliable responses.

Nevertheless, within the evaluated design spaces, the nitrogen flow rate, V_f was identified as the dominant factor in determining high recovery efficiency and reducing operating cost, whereas I_R was found to be critical in achieving high recovery, though at an increased cost. This increased cost is compensated, however, by the elevated *FR*. No significant interaction effects were observed. In 2012 when investigating the recovery of acetone, dichloromethane and ethyl formate using microporous carbon in a TSA process, (Ramalingam et al., 2012) employed a factorial design. In this case, nitrogen temperature (X_1) and superficial gas velocity (X_2) were optimised to maximise regeneration efficiency (R_E) and minimise operating cost. The two levels considered for X_1 were 130 and 170°C and for gas velocity (v), 0.10 and 0.17 m/s in a 2^2 design using Minitab. For each VOC, v was found to be the most significant factor with regards to R_E, with the interaction effect greater in the case of acetone. An increase in X_1 resulted in a reduction in OP_{EUR} for all cases.

The fractional factorial design has been deployed by (Rodríguez-Mosqueda et al., 2018) to conduct a parametrical study on direct air CO_2 capture using a hydrated potassium carbonated sorbent supported on an activated carbon honeycomb. With a view to investigate the impacts T_{ads} (X_1, 20 and 40°C), water vapour pressure of air (P_w, X_2, 5 and 17 mbar) and air flow rate (X_3, 5 and 15 L/min), an AC monolith, coated in K_2CO_3 and hydrated by moist nitrogen, was tested *via* a fractional factorial design of experiments. The centre points were chosen such that each factor represents the middle value (*i.e.* 30°C, 12 mbar and 10 L/min) in the interest of exposing curvature in the response of adsorption capacity. Repeatability of results was evaluated by conducting the centre point in triplicates; the adsorption data was then analysed using Minitab. The fitted equation presented a standard deviation of 4.2% and an R^2 value of 97.85% with the response being influenced only by X_3, X_1 X_2 and X_2 with latter exhibiting the strongest effect. When conducting the triplicate centre point, a reduction in the response was observed indicating a 4.8% loss of adsorbent capacity. The main effects plot for X_2 and X_3 indicated a linear relationship with the response. With regards to the interaction between X_1 and X_2, the plot elucidated a dynamic relationship where at low P_w the capture capacity increased with T_{ads}, whereas the opposite was observed at high P_w. Interestingly, an increase in temperature alone was not observed to significantly disadvantage the capture efficiency which would be expected due to the shifting of the chemical equilibrium in an exothermic process. This unconventional observation, however, was determined to be a result of the evaporation and desorption of water that occurs concurrently with CO_2. The cooling effect as result of evaporation is obviously more prominent at elevated temperatures, which might also explain why T did not feature as a significant factor in the analysis.

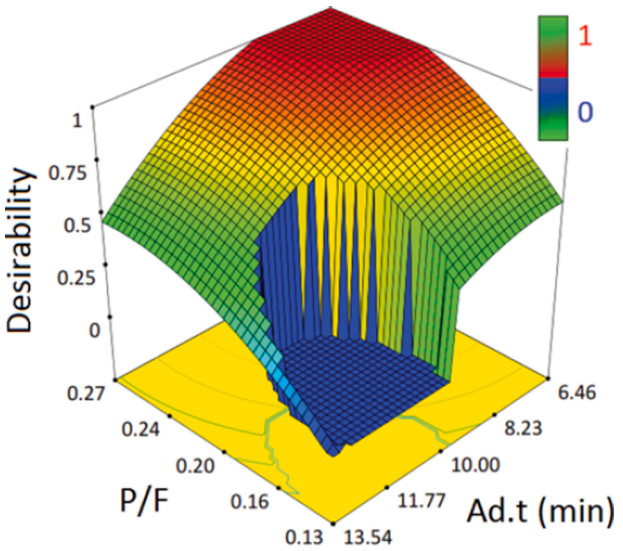

Fig. 11. – Response surface plot of desirability vs the P/F ratio and τads (Ad.t on the graph) in the one-column PSA process (adopted from (Saberimoghaddam and Nozari, 2017)).

4.1.2. Central Composite DoE

The central composite design of experiment has featured in the experimental and statistical study of hydrogen purification *via* pressure swing adsorption (PSA) (Saberimoghaddam and Nozari, 2017) with a view to develop a statistical process model without the need for complex partial differential equations and involved procedures. Here, the PSA process was modelled and optimised to maximise the adsorption of CO_2 from a binary H_2/CO_2 mixture and revealed distinct second-order polynomial equations that could predict the purity (%), recovery (%) and productivity of hydrogen (lit/grs) with R^2 values of over 0.99. The effects of purge to feed ratio (P/F) and τ_{ads} on hydrogen purity, productivity and recovery as well as their interactions were assessed. In this case, P/F ratio (0.10 – 0.30) and τ_{ads} (5 – 15 min) are the independent variables; thirteen experiments were conducted in total due to the presence of 5 central replicates. The authors identified that effects of P/F, τ_{ads}, $(P/F)^2$ and $(\tau_{ads})^2$ were all significant ($P < 0.0001$) whilst the statistical models for the three responses: purity, recovery and productivity possessed F-values of 204.91, 376.00 and 483.92, respectively. Additionally, R-squared values for each model were above 0.99 indicating good approximation of the experimental data which is corroborated by Adeq Precision measures (which measure the signal to noise ratio) above 4. Regarding the effect of each independent variable, the authors identified a number of notable relationships within the PSA process. An increase in P/F was observed to increase the purity whilst decreasing both recovery and productivity whereas when increasing τ_{ads} purity remained constant until $Ad.t = 10$ min after which it began to decline due to fresh adsorbent availability being finite. However, above 10 min, each response saw a decrease. By optimising the PSA process under two conditions (in range or maximise), seven cases were identified; qualitative appraisal of the seven cases can be used to identify the optimum. Due to this, an overall desirability (D) was employed as a parameter to select the optimum condition; when maximisation of responses is required, the overall desirability and desirability for each response are defined as below (Saberimoghaddam and Nozari, 2017), (Gunst et al., 1996):

$$D = \left(d_1^{r_1} \times d_2^{r_2} \times \ldots \times d_m^{r_m}\right)^{\frac{1}{r_1+r_2+\ldots+r_m}} \tag{10}$$

$$d_i = \left(\frac{y_i - L}{T - L}\right)^w \tag{11}$$

when a response is in range, the desirability is defined as shown below

(Saberimoghaddam and Nozari, 2017):

$d_i = 0$ if response < low value
$d_i = 1$ if response varies from low to high
$d_i = 0$ if response > high value

Where D is the overall desirability, d_i is desirability for each response, r_i represents the importance of each response which varies from 2 to 5 and w is the weight of each response; T and L represent the maximum and minimum possible value for the responses, respectively; y_i is the optimum value. A response surface was plotted (Fig. 11) representing the overall desirability (D) against P/F and τ_{ads}, when purity was maximum, and recovery and productivity were in range. The surface of $D = 1$ provided a flexible PSA process at the maximum purity at low P/F and high τ_{ads}. An overall desirability of 0.884 was achieved when maximising all responses: $P/F = 0.2$, τ_{ads}= 10.42 min, purity = 96.31, recovery = 54.31 and productivity = 3.37×10^{-5}.

In the application of acid gas removal by sawmill residue-derived biochar, (Bamdad et al., 2019) employed a CCD coupled with RSM to determine the optimum conditions for maximising acid gas (CO_2) adsorption and for assessment of the process itself. The adsorption parameters considered included T_{ads} (X_1, 20 to 80°C), inlet feed flow rate (X_2, 60 to 200 mL/min) and CO_2 concentration (X_3, 20 to 100 %, (v/v)), whilst the response evaluated was the adsorption capacity. In total, 20 experiments were conducted. It was observed that when increasing the inlet flow rate, the bed became saturated more quickly due to an increased mass of CO_2 entering the system; the mass transfer zone also became narrower whilst the mass transfer coefficient increased as a result of an increase in the corresponding Reynolds number. Contrastingly, the equilibrium capacity of the bed was seen to increase at lower inlet flow rates due to an elevated residence time. When increasing the adsorption temperature, the breakthrough time was seen to decrease yet by decreasing CO_2 concentration in the feed stream, a slight increase in breakthrough time was realised since binding sites become saturated more quickly at elevated adsorbate concentrations (Bamdad et al., 2019). A decrease to adsorbent CO_2 concentration in the inlet gas stream will also act to decrease the overall driving force of adsorption, hence increasing the time required for breakthrough and ultimately decreasing adsorbent capacity (O'Mahony et al., 2002). ANOVA tests were able to determine that the interactions between $X_1 X_2$ and $X_1 X_3$ and both X_1 and X_3 have a significant effect on the adsorption capacity. The model itself was significant and presented an F-value of 46.88 with an Adeq value of 23.354 demonstrating good model discrimination.

(Vohra et al., 2020) employed date palm-tree branch-based AC to treat gaseous toluene streams under varying dynamic flow conditions using a 6.5 mm ID column at atmospheric pressure and room temperature. The authors investigated the effect of influent gas flow rate (X_1, 2 – 3 slpm), AC bed depth (X_2, 4 – 6 cm) and influent gas concentration (X_3, 10 –20 ppmv) on the breakthrough (BT) and exhaustion time (ET) using a CCD design with one centre point. All of the studied variables within their ranges, presented statistically significant influence on the responses (p-values < 0.05) and the Adeq precision values were 19.3374 and 25.5566 for the BT and ET models, respectively, which are indicative of a good model fit. The respective models were also assessed based on the assumptions of normality and random variation of the residuals, the plots confirmed the assumptions and hence the respective normality and randomness results indicated model validity. Their results depict a decrease in both BT and ET when increasing the flow rate as a result of a reduced residency time leading to a reduced bed efficiency and an early breakthrough and exhaustion. Additionally, a higher influent toluene concentration from was shown to reduce both BT and ET irrespective of gas flow rate. This is indicative of the AC employed which possesses a fixed amount of adsorption sites and specific surface area; an increase in concentration accelerates adsorbent saturation.

(Baytar et al., 2020) too, studied the effect of process parameters on the adsorption of toluene. In this work, though, the adsorption of another VOC, benzene was also considered. Employing an experimental setup with a glass reactor of 16 cm in height and 0.9 cm ID, the effect of τ_{ads} (X_1, 14.66 – 90.34 min), initial concentration (X_2, 9.27 – 22.72 ppm) and T_{ads} (X_3, 16.48 – 58.52°C) was evaluated on the adsorption capacity of benzene and toluene (mg/g). A total of 20 experiments were defined with 6 replications at the central point for each response; statistical significance was measured with an F-value ($p < 0.05$) at a 95 % confidence level. The correlation coefficients (R^2) of the proposed model equations were all in the range 0.95 – 0.99 indicating successful representation of the experimental data. In this work, all independent variables were deemed significant on the two responses, with τ_{ads} presenting being most impactful on both benzene and toluene adsorption. The Adeq precision measures were 81.31 and 49.82 for benzene and toluene adsorption capacities. Multiple linear regression analysis of the data resulted in quadratic polynomial equations for each response which were assessed through ANOVA and were found to be accurate representations of gas-phase adsorption of the VOCs in the presence of AC. The response surfaces depicted an increase in capacity for both VOCs when increasing τ_{ads} which can be explained by the fact that adsorption capacity is a function of time (de Luna et al., 2013), and that the increase in the number of gas-phase adsorbate molecules acts to accelerate access to the adsorption equilibrium state (Hameed and El-Khaiary, 2008). When increasing initial concentration, no significant change in capacity was observed due to the finite availability of specific surface area and adsorption sites (Vohra, 2015). When considering time and temperature, as expected with the exothermic nature of physical adsorption, capacity decreased with an increase in temperature and increased with time for a constant initial concentration. For a constant τ_{ads}, capacities decreased with increasing T_{ads}; however, no significant change was identified when increasing initial concentration since the total amount of VOC adsorption onto AC is constant. The optimum process conditions for benzene adsorption were defined at an τ_{ads} of 74.98 minutes, a concentration of 16.68 ppm and a T_{ads} of 26.97°C resulting in a capacity of 437.76 mg/g. In the case of toluene, these conditions were 73.26 minutes, 18.46 ppm and 29.8°C, resulting in a capacity of 512.03 mg/g.

4.1.3. Box-Behnken DoE

The Box-Behnken Design of experiment has also featured in the assessment of gas-phase toluene removal with granular activated carbon in the work of (Gupta and Kumar, 2020). The experimental setup involved a 0.1 m high column with an ID of 0.05 m; breakthrough time was defined at an effluent toluene concentration equal to 5% of the inlet toluene concentration. The three variables studied included bed height (X_1, 0.015 – 0.025 m), initial concentration (X_2, 7000 – 11500 ppm) and flow rate (X_3, 35 – 106 ml/min); the response was defined as the fraction of the bed utilised until the measured breakthrough time, thus, leading to 15 experiments (as both P and X were 3). The experimental data was fitted to a second-order polynomial. The adequacy of the proposed model was evaluated using ANOVA. With an F-value of 247.98 and a p-value of < 0.05, the model was clearly significant. The residual analysis clearly indicated that the model accurately described the experimental domain. The analysis also elucidated the statistical significance of all three parameters on the response, while the square and interaction effects presented a statistically insignificant influence. Optimisation in Minitab identified a maximum in the response, fraction of bed utilised until breakthrough of 0.774 at a bed height of 0.025 m, an inlet concentration of 11500 ppm and a flow rate of 35 ml/min. When conducting a confirmation experiment under these conditions, the response was found to be 0.81 indicating a good agreement with the model.

In the optimisation of CO_2 adsorption by (Baldovino et al., 2017), T_{ads} (X_1, from 40 to 120°C) and inlet gas flow rate (X_2, from 100 to 300 ml/min) also featured as the investigated variables alongside adsorbent (nitrogen-functionalised graphene-oxide) loading (X_3, from 4 to 8 mg). . Using a modified TGA-equipment, the modified graphene oxide was evaluated for CO_2 adsorption using 15 pre-defined experiments with the response Y defined as the amount of CO_2 adsorbed ($mmol_{CO2}$). The

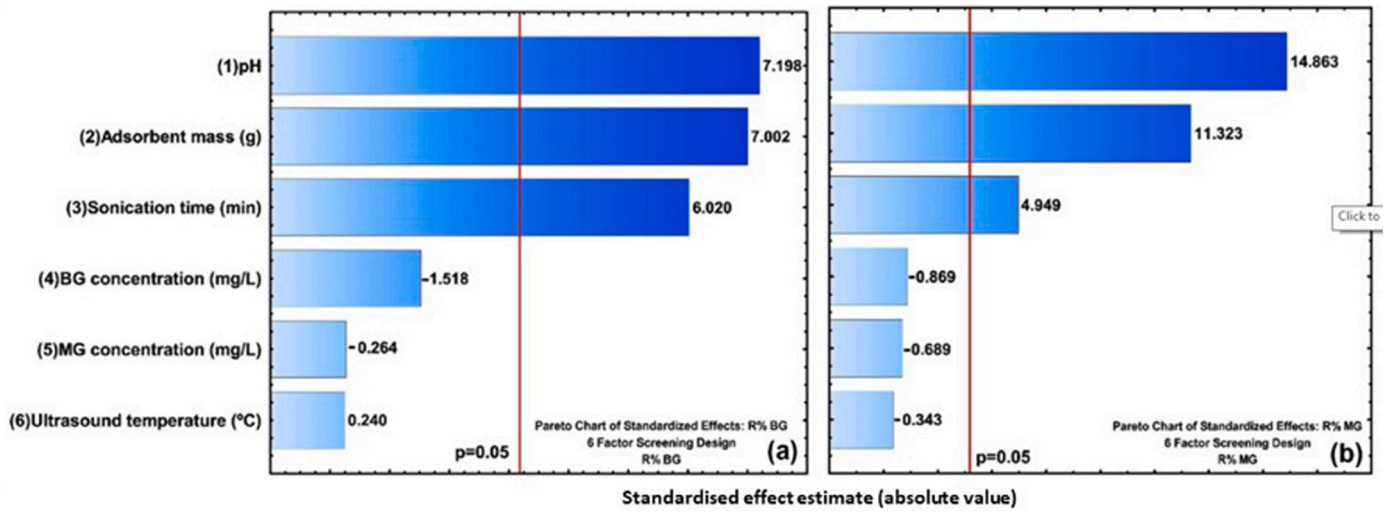

Fig. 12. – Pareto chart of parameters effects on the removal efficiency for (a) BG and (b) MG. (Asfaram et al., 2017).

optimum points were found at 80°C, 100 ml/min and 8 mg providing an uptake of 0.0063 $mmol_{CO2}$. If we first consider the optimum T_{ads}, this is contrary to the generally accepted ideal temperature for physical adsorption, but you must consider that there exists nitrogen-functionalities on the adsorbent surface which require elevated temperatures to interact with the CO_2, hence, 80°C is likely the ideal temperature for a cooperative contribution to adsorption from both the physical and chemical interactions. Although unlikely to inform those considering industrial deployment of this modified graphene oxide, the results did expose several things that must be considered when investigating novel materials for CO_2 adsorption using TGA equipment. The optimum values for both the adsorbent loading and gas flow rate are most likely a result of the experimental setup. A larger loading simply exposes a greater surface area for adsorption to take place, whereas an elevated flow rate just increases the throughput of gas in the fixed TGA furnace volume thus reducing residency time and hence, reducing the quantity adsorbed. The proposed quadratic model revealed by the RSM presented a predicted optimum response with a 1.59 % error.

4.2. Optimisation of Adsorbents' Capacity via Variation of Process Conditions; Aqueous Media

4.2.1. Factorial DoE

A 2^4 full factorial design has been applied to optimise the adsorption of many pollutants including MB using AC synthesised from cashew nut shells (Subramaniam and Kumar Ponnusamy, 2015). The experimental design in this study, however, also contained nine replicates at the centre point and eight experiments at axial points, resulting in 33 experiments conducted in total. The independent process variables were pH (X_1, 2 – 10), adsorbent dose (X_2, 0.5 – 3 g/L), initial dye concentration (X_3, 50 – 250 mg/L) and τ_{ads} (X_4, 60 – 120 min). Minitab 14 software was used to estimate the response of the dependent variable. The optimum conditions for maximum MB removal were 10, 2.18 g/L, 50 mg/L and 63 min for pH, adsorbent dose, initial dye concentration and τ_{ads}, respectively. It was observed that the adsorption capacity of MB is significantly reduced when the pH is very acidic (≤ 2). At low pH MB is positively charged and therefore, competitive adsorption would be observed between the cationic dye and the H^+ ions. Additionally, in acidic conditions, the pH is lower than the point of zero charge of the adsorbent causing the surface to become positive. Consequently, the electrostatic repulsion between the adsorbent and the dye increases, therefore, decreasing the adsorption capacity. The student t-test was applied to determine the significance of the parameters. All factors were realised to be significant due to their high t numbers and p-values smaller than 0.05. ANOVA was applied to determine the significance of the model. The large F-value of 161.8 and p-value of < 0.0001 indicated that the model was highly significant and could adequately represent the relationship between the variables and the response at a 99 % confidence level. The optimisation of adsorbent dosage and contact time on removal percentage was studied using RSM. The maximum removal was achieved when the adsorbent dose and τ_{ads} were in the region of 1.4 – 2.2 g/L and 60 – 90 minutes, respectively.

A 2^5 full factorial design has been less commonly used to optimise chromium (VI) adsorption using a granular AC (Halder et al., 2015). This experimental matrix was applied to investigate the effects of pH, AC dose, contact time, initial concentration and temperature on percentage removal. The method employed ANOVA and RSM to determine the optimum removal efficiency of 96.33 %, which was achieved when the conditions were as follows: pH 4.0, AC dose 1.6 g/L, contact time 40 min, initial concentration 200 mg/L and temperature of 35°C.

4.2.2. Central Composite DoE

Many studies have been undertaken to optimise the adsorption of pollutants, when considering up to three factors; however, when there is a lack of knowledge about the system in question, there could be a large number of potential factors. Preliminary screening methods such as Placket-Burman analysis can be applied to determine factors with significant contribution to the output. Pareto charts are a good visual method to identify significant factors and/or interactions involved in a design optimisation study. This is achieved by arranging the absolute values of the target factors (calculated by statistical software) in a descending order (Antony, 2014). The key component of the graph is the reference line; any factors exceeding this limit are deemed to be significant, whereas the factors below are not. For example, (Asfaram et al., 2017) used this method to consider six factors: pH, adsorbent mass, sonication time, brilliant green (BG) and malachite green (MG) concentration and ultrasound temperature, discovering the former three factors to be significant using Pareto charts (Fig. 12). The factors were studied on five levels and a total of 14 experimental runs. The optimum conditions were found to be a pH of 7.0, an adsorbent dosage of 0.02 g and an ultrasonication time of 3 minutes. At optimum conditions, the removal percentages for MG and BG were 99.5 % and 99.0 %, respectively.

ANOVA revealed that pH had the most significant impact on the removal percentage of both BG ($f = 793.8$, $p < 0.0001$) and MG ($f = 1934.0$, $p < 0.0001$). It was observed that adsorption capacity decreases with decreasing pH. As mentioned in section 4.2.1, this is due to competitive adsorption between the dyes and H^+ ions and increased

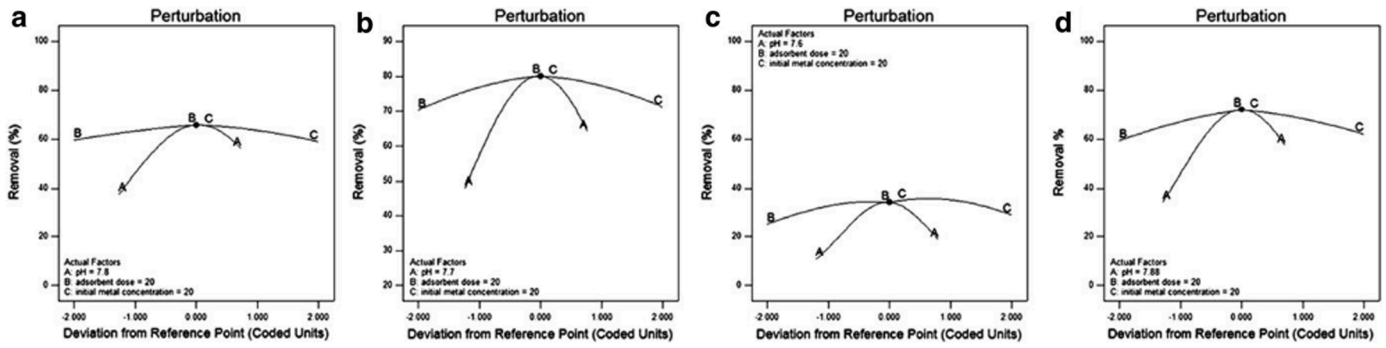

Fig. 13. – Perturbation plot for the adsorption process. a Hg(II) removal by MWCNTs-COOH, b Hg(II) removal by MWCNTs-f, c As(III) removal by MWCNTs-COOH, and d As(III) removal by MWCNTs-f (Alimohammady et al., 2018).

electrostatic repulsion. Analysis of combined effects revealed that pH and sonication time had a significant impact on BG adsorption ($f = 151.9$, $p = 0.0003$), whereas MG adsorption was considerably affected by the interaction between adsorbent mass and sonication time ($f = 80.18$, $p = 0.0002$). Similar to BG adsorption, the maximum MG adsorption was achieved when both of the interacting factors were at their maximum values. RSM determined that the maximum removal percentage was achieved in the region defined by the highest adsorbent mass and sonication time.

Adsorption of heavy metals and dyes using functionalised multi-walled carbon nanotubes (MWCNT) was optimised using CCD (Alimohammady et al., 2018, Mahmoodi et al., 2020, Bandari et al., 2015). The heavy metal studies were similar in the fact that they both investigated adsorbent dose, pH and initial ions concentration. (Alimohammady et al., 2018) investigated the three factors on five levels, while (Mahmoodi et al., 2020) investigated an additional factor of contact time, on 3 levels. Both studies employed Design-Expert to determine the experimental design and statistically assess the data. The former study consisted of 20 experimental runs, whereas the later required an additional 10 experiments. Both studies applied ANOVA to determine the significant factors. (Alimohammady et al., 2018) reported that pH had the greatest impact on both the adsorption of Hg(II) and As(III). In contrast, for Cd(II) the concentration was found to be the most significant factor in the latter study (Mahmoodi et al., 2020). RSM was applied in both cases to gain an understanding of the combined effects of the variables and determine the optimum conditions for adsorption; however, the former (Alimohammady et al., 2018) further analysed the data using perturbation plots (Fig. 13). In all cases, pH displayed a sharp curvature indicating sensitivity of this variable. The plots also indicated that maximum removal efficiency was achieved when adsorbent dose was at the maximum level.

The value of the pH determines the dominant species present in the solution, for example, at $pH < 3$, Hg^{2+} is the dominant species, whereas $Hg(OH)_2$ becomes dominant at $pH \geq 6$. When the pH is raised to above 6, the adsorption capacity is substantially increased due to hydrogen bonding between mercuric hydroxide and the carboxylate groups on the surface of the MWCNTs. Additionally, at lower pH there is strong competition between H^+ and the metal ions on the adsorption sites, reducing adsorption capacity. The optimum conditions for the adsorption of Hg(II) and As(III) were found to be a pH of 7-8, an adsorbent dosage of 20 mg, and an initial ionic concentration of 20 ppm. The optimum conditions for Cd(II) adsorption, were 0.02 g, 10.69 mg/l, 30.45 min and 6.37 for adsorbent dose, Cd(II) concentration, contact time and pH, respectively.

Other researchers have optimised the removal of organophosphorus pesticides (azinphos methyl, chlorpyrifos, malathion, and parathion) using CCD (Wanjeri et al., 2019). MWCNTs fixed onto the surface of a magnetic silica substrate (Fe_3O_4@SiO_2). The experimental method was designed using Statistica version 8. Three experimental factors were considered on three levels, namely, pH (X_1, 3 – 11), adsorbent dosage (X_2, 6 – 80 mg) and τ_{ads} (X_3, 6 – 60 min). The optimum conditions were found to be an adsorbent dosage of 80 mg, a pH of 7 and a contact time of 6 min, giving a maximum removal efficiency of 89.8, 95.9, 99.8, and 99.2 %, for azinphos methyl, chlorpyrifos, malathion, and parathion, respectively. Following ANOVA, dosage was determined to be of most significance for azinphos methyl, chlorpyrifos and parathion, whereas pH was the most significant factor for malathion. The acidity of the solution was still significant for azinphos methyl adsorption (though, had little impact on chlorpyrifos and parathion). This was attributed to the decomposition of azinphos methyl and malathion within acidic and alkaline solution, affecting their recovery. Nevertheless, malathion is most sensitive to pH due to the absence of a benzene ring within the structure, leading to a lack of π-π stacking interactions at higher pH and consequently, lower percentage recoveries. Removal efficiency increased with increasing dosage for all organophosphorus pesticides due to the increase in available active sites for adsorption. Additionally, extraction time was shown not to impact sorption of the evaluated pesticides.

4.2.3. Box-Behnken DoE

BBD has been employed to optimise the removal percentage of MB using chemically-activated carbon (Jawad et al., 2020), (Jawad and Abdulhameed, 2020). One study (Jawad et al., 2020), applied an optimisation process consisting of 29 experimental runs with three levels, five centre points and four parameters investigating the impacts of adsorbent dose (X_1, 0.02 – 0.08 g), pH (X_2, 4 – 10), T_{ads} (X_3, 30 – 60°C) and τ_{ads} (X_4, 30 – 120 min). All factors were found to be statistically significant when analysing the data using ANOVA ($p < 0.05$). Dosage was found to have the greatest effect on removal percentage ($f = 135.19$, $p < 0.0001$), temperature was the least impactful parameter ($f = 5.17$, $p = 0.0393$). When considering combined effects, however, only the interaction between X_1 and X_2 was statistically significant ($f = 10.21$, $p = 0.0065$). RSM was utilised to further study X_1 X_2, depicting a positive correlation between dosage and pH with removal percentage reaching a maximum when both factors are at the highest value. The phenomenon can be explained by considering the point of zero charge of that AC (6.8). At pH greater than 6.8 the adsorbent acquires a negative charge, hence, an enhanced electrostatic attraction between the adsorbent and the cationic dye resulting in greater removal percentage.

Several studies have applied BBD to optimise the removal of heavy metals (Azari et al., 2015), (Adetoro and Ojoawo, 2020). (Azari et al., 2015) applied BBD to optimise the removal percentage of Ni(II), Co(II) and Cd(II) using a magnetite-AC composite. The method was planned using Design Expert software (version 8.0), consisting of 46 experimental runs to investigate the following factors on three levels: pH, τ_{ads}, T_{ads}, adsorbent dose and initial concentration of metal ions. RSM was applied to investigate the effects of pH and temperature and the former was found to be the significant parameter. This phenomenon was

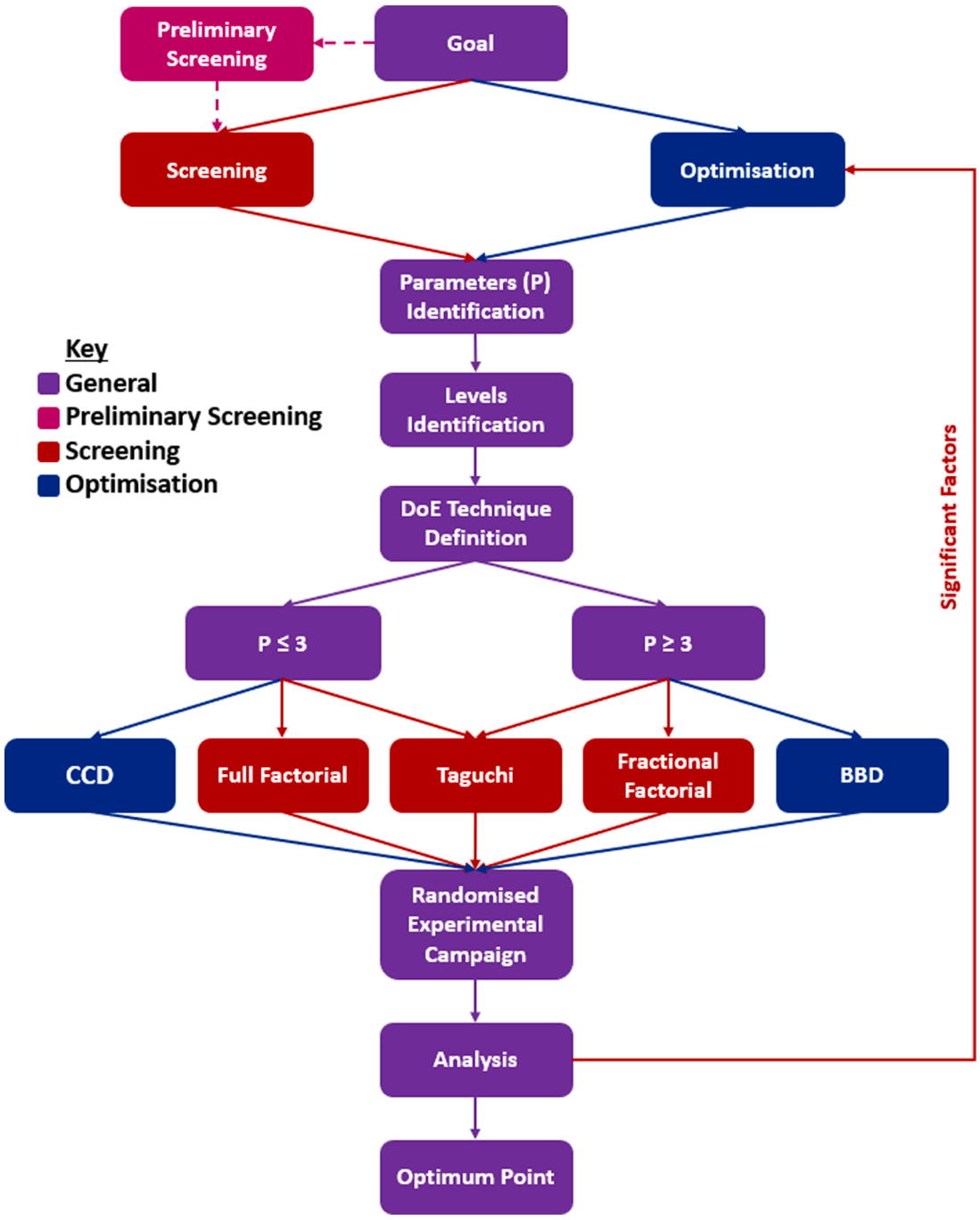

Fig. 14. – Simplified algorithm for DoE selection and execution.

attributed to electrostatic forces between the adsorbent and metal ion as when the pH is acidic, the surface of the adsorbent is positive leading to electrostatic repulsion between the metal ions and the positive surface. The surface of the adsorbent becomes ionised as the pH is increased leading to increased electrostatic attraction and removal percentage. The 3D surface plots also revealed the τ_{ads} and initial ion concentration to be inversely related, therefore, maximum removal percentage was achieved when τ_{ads} was at the highest value and initial concentration was at the minimum (due to increased competition for active sites on the adsorbent surface when the concentration of ions was elevated). Adsorbent dosage and τ_{ads} were also studied using RSM, depicting maximum removal efficiency at the greatest level of both factors. ANOVA was applied to determine the significance of the model. The F-values for Ni(II), Co(II) and Cd(II) were 83.80m 69.05 and 56.09, respectively All p-values were < 0.0001, indicating that the models for all ions were significant.

5. Conclusions and Recommendations

Experimental work is often tedious, requiring myriad time and resources. However, intelligent designs of experimental campaigns can not only alleviate this burden but also provide valuable insight into the governing forces, their prominence and impacts on the response variable. Within academia, the powerful DoE techniques have been mostly overlooked, leading to usage of additional time and resources as well as missing the various possible parameter interactions that may greatly impact the outcome of the process. This might be attributed to the fact that these powerful optimisation tools are, perhaps, not fully understood

and have been, for part, overlooked within academia.

Here, we have endeavoured to facilitate a better understanding of some of the most popular DoE techniques (*via* a description backed up with a simple visualisation, outline of their benefits and drawbacks, proposed applications, followed by an overview of the most prominent data analysis tools as well as best practices) in order to maximise implementation of advanced experimental designs within the academic domain of chemical and environmental engineering, which was then followed by examples and discussion of the results and their interpretations within the domain of carbonaceous adsorbents' synthesis and application. This review paper aims to help bridge the gap between commonly employed optimisation DoE tools and their deployment in academic research to improve sorbent uptake capabilities and the associated process performance in environmental applications. Unfortunately, the vast range of carbonaceous adsorbents precursors, their proposed application (both in terms of adsorption media, adsorbate and process envelope) and processing/activation techniques prohibits a blanket approach towards optimisation. Nevertheless, in terms of sorbent production, τ_{act} and T_{act} coupled with IR for chemical activation (and potentially their interactions) are more often than not found to be the most impactful parameters in terms of sorption capacity enhancement and porosity development (within the confinements of their (respective) appropriate levels). In terms of adsorption process optimisation, the feed conditions (whether adsorbate concentration and/or flow rate) and the process/experimental conditions (time, pH, temperature, pressure and etc.) as well as their interactions are normally found to be statistically significant. The exact parameters and levels would vary greatly depending on the optimisation goal (e.g. maximum removal efficiency or optimised cost), the materials and methods as well as the experimental campaign goal itself.

The authors urge the operators to plan and then evaluate critically their proposed experimental campaign *in primis;* prior to execution, and to identify the appropriate DoE technique based on desired outcome (goal of the study) as well as the number of parameters (and levels) involved. The choice of these input variables could be informed based on previous works or literature on similar adsorbents, adsorbates, processes and etc. The levels should endeavour to encompass the maximum range possible (that would result in high quality data (e.g. avoiding data loss points, equipment constraints or clearly ludicrous conditions)), whilst simultaneously striving to keep the step size as small as practically possible. Additionally, prior to optimisation, if the process is not yet well understood, (pre)screening studies are recommended. These may well inform (or even be incorporated into) the next experimental design. A simplified flow chart is depicted in Fig. 14 to help practitioners visualise the process of adopting and carrying out an experimental campaign utilising DoE technique to their full potential.

It is a good practice to avoid misusing designs, i.e. *screening parameters with a CCD* or *employing small 2-level factorial designs to study high-order interactions*. Additionally, avoiding simple 2-level designs (by adding centre points or increasing the number of levels) as well as randomising the trials are advised. The former assists with determining curvilinear relationships within the design space, while the latter decreases the impact of noise on the system. Moreover, operators have to keep in mind that the *mathematical* optimum might be unattainable or uneconomical in real-world applications.

Wide implementation of DoE techniques would not only increase the pace at which evaluations and academic studies are carried out, but it would also improve the optimisation of the associated processes. Consequently, this would allow for accumulation of more data (for instance, the vast importance of parameter interactions on the operation of a system as a whole and its actual demonstration as opposed to theoretical concepts) and fundamental understanding, whilst utilising fewer resources and therefore, paving the way for the conduction of accelerated yet more efficient research.

Compliance with Ethical Standards

We would like to confirm that there has been no conflict of interests among the authors of this manuscript, and that no research involving human participants and/or animals have been taken in this work.

Declaration of Competing Interest

The authors declare that they have no known competing financial interests or personal relationships that could have appeared to influence the work reported in this paper.

Acknowledgement

This work has been funded by the UK Engineering and Physical Sciences Research Council (EPSRC) under the project titled "Multi-physics and multiscale modelling for safe and feasible CO_2 capture and storage - EP/T033940/1", and *via* the UK Carbon Capture and Storage Research Centre (EP/P026214/1) through the flexible funded research programme "Techno-economics of Biomass Combustion Products in the Synthesis of Effective Low-cost Adsorbents for Carbon Capture". The UKCCSRC is supported by the Engineering and Physical Sciences Research Council (EPSRC), UK, as part of the UKRI Energy Programme. The authors are grateful to the Research Centre for providing this funding.

Bibliography

Abdel-Ghani, N.T., El-Chaghaby, G.A., Elgammal, M.H., Rawash, E.S.A., 2016. Optimizing the preparation conditions of activated carbons from olive cake using KOH activation. Xinxing Tan Cailiao/New Carbon Mater 31 (5), 492–500.

Adetoro, E.A., Ojoawo, S.O., 2020. Optimization study of biosorption of toxic metals from mining wastewater using Azadirachta indica bark adsorbents. Water Sci. Technol. 82 (5), 887–904. Sep.

Alam, M.Z., Ameem, E.S., Muyibi, S.A., Kabbashi, N.A., 2009. The factors affecting the performance of activated carbon prepared from oil palm empty fruit bunches for adsorption of phenol. Chem. Eng. J. 155 (1–2), 191–198. Dec.

Alaoui, A., Kacemi, K.E.L., Ass, K.E.L., Kitane, S., 2015. Application of box-behnken design to determine the optimal conditions of reductive leaching of MnO2 from manganese mine tailings. Trans. Indian Inst. Met. 68 (5).

Alimohammady, M., Jahangiri, M., Kiani, F., Tahermansouri, H., 2018. Design and evaluation of functionalized multi-walled carbon nanotubes by 3-aminopyrazole for the removal of Hg(II) and As(III) ions from aqueous solution. Res. Chem. Intermed. 44 (1), 69–92. Jan.

Antony, J., 2003. Fundamentals of Design of Experiments. Design of Experiments for Engineers and Scientists. Elsevier Ltd, pp. 6–16.

Antony, J., 2014. A Systematic Methodology for Design of Experiments. Design of Experiments for Engineers and Scientists. Elsevier, pp. 33–50.

Asfaram, A., Ghaedi, M., Hajati, S., Goudarzi, A., Dil, E.A., 2017. Screening and optimization of highly effective ultrasound-assisted simultaneous adsorption of cationic dyes onto Mn-doped Fe3O4-nanoparticle-loaded activated carbon. Ultrason. Sonochem. 34, 1–12. Jan.

Azari, A., et al., 2015. Rapid and efficient magnetically removal of heavy metals by magnetite-activated carbon composite: a statistical design approach. J. Porous Mater. 22 (4), 1083–1096. Aug.

Baldovino, F.H.B., Dugos, N.P., Roces, S.A., Quitain, A.T., Kida, T., 2017. Process optimization of carbon dioxide adsorption using nitrogen-functionalized graphene oxide via response surface methodology approach. ASEAN J. Chem. Eng. 17 (2), 106–113.

Bamdad, H., Hawboldt, K., MacQuarrie, S., Papari, S., 2019. Application of biochar for acid gas removal: experimental and statistical analysis using CO 2. Environ. Sci. Pollut. Res. 26 (11), 10902–10915.

Bandari, F., Safa, F., Shariati, S., 2015. Application of Response Surface Method for Optimization of Adsorptive Removal of Eriochrome Black T Using Magnetic Multi-Wall Carbon Nanotube Nanocomposite," Arab. J. Sci. Eng. 40 (12), 3363–3372. Dec.

Basheer, A.O., et al., 2019. Synthesis and Characterization of Natural Extracted Precursor Date Palm Fibre-Based Activated Carbon for Aluminum Removal by RSM Optimization. Processes 7 (5), 249. Apr.

Baytar, O., Şahin, Ö., Horoz, S., Kutluay, S., 2020. High-performance gas-phase adsorption of benzene and toluene on activated carbon: response surface optimization, reusability, equilibrium, kinetic, and competitive adsorption studies. Environ. Sci. Pollut. Res. 27 (21), 26191–26210.

Bergna, D., Hu, T., Prokkola, H., Romar, H., Lassi, U., 2020. Effect of Some Process Parameters on the Main Properties of Activated Carbon Produced from Peat in a Lab-Scale Process. Waste and Biomass Valorization 11 (6), 2837–2848.

G. E. P. Box and K. B. Wilson, "On the Experimental Attainment of Optimum Conditions," J. R. Stat. Soc. Ser. B, 1951.

Chen, Y.D., Chen, W.Q., Huang, B., Huang, M.J., 2013. Process optimization of K2C2O4-activated carbon from kenaf core using Box-Behnken design. Chem. Eng. Res. Des. 91 (9), 1783–1789. Sep.

R. Davis and P. John, "Application of Taguchi-Based Design of Experiments for Industrial Chemical Processes," Stat. Approaches With Emphas. Des. Exp. Appl. to Chem. Process., 2018.

de Luna, M.D.G., Flores, E.D., Genuino, D.A.D., Futalan, C.M., Wan, M.W., 2013. Adsorption of Eriochrome Black T (EBT) dye using activated carbon prepared from waste rice hulls-Optimization, isotherm and kinetic studies. J. Taiwan Inst. Chem. Eng. 44 (4).

Dos Reis, G.S., et al., 2016. The use of design of experiments for the evaluation of the production of surface rich activated carbon from sewage sludge via microwave and conventional pyrolysis. Appl. Therm. Eng. 93, 590–597.

Ekrami, E., Dadashian, F., Soleimani, M., 2014. Waste cotton fibers based activated carbon: Optimization of process and product characterization. Fibers Polym 15 (9), 1855–1864.

Ferreira, S.L.C., et al., 2007. Statistical designs and response surface techniques for the optimization of chromatographic systems. Journal of Chromatography A 1158 (1–2).

Gao, Y., et al., 2015. Optimization of high surface area activated carbon production from Enteromorpha prolifra with low-dose activating agent. Fuel Process. Technol. 132, 180–187.

Garba, Z.N., Abdul Rahim, A., Hamza, S.A., 2014. Potential of Borassus aethiopum shells as precursor for activated carbon preparation by physico-chemical activation; Optimization, equilibrium and kinetic studies. J. Environ. Chem. Eng. 2 (3), 1423–1433. Sep.

García, S., Gil, M.V., Martín, C.F., Pis, J.J., Rubiera, F., Pevida, C., 2011. Breakthrough adsorption study of a commercial activated carbon for pre-combustion CO2 capture. Chem. Eng. J. 171 (2), 549–556.

Ghasemi, A., Zahediasl, S., 2012. Normality tests for statistical analysis: A guide for non-statisticians. Int. J. Endocrinol. Metab. 10 (2), 486–489. Apr.

Gunst, R.F., Myers, R.H., Montgomery, D.C., 1996. Response Surface Methodology: Process and Product Optimization Using Designed Experiments. Technometrics 38 (3).

Gupta, K.N., Kumar, R., 2020. Kinetic modeling and optimization of fraction of bed utilized for the gaseous phase removal of toluene in fixed bed adsorption column: Response surface methodology. Sep. Sci. Technol. 55 (6), 1062–1077.

Halder, G., Dhawane, S., Barai, P.K., Das, A., 2015. Optimizing chromium (VI) adsorption onto superheated steam activated granular carbon through response surface methodology and artificial neural network. Environ. Prog. Sustain. Energy 34 (3), 638–647. May.

Hameed, B.H., El-Khaiary, M.I., 2008. Equilibrium, kinetics and mechanism of malachite green adsorption on activated carbon prepared from bamboo by K2CO3 activation and subsequent gasification with CO2. J. Hazard. Mater. 157 (2–3).

Hoseinzadeh Hesas, R., Arami-Niya, A., Wan Daud, W.M.A., Sahu, J.N., 2013. Preparation of granular activated carbon from oil palm shell by microwave-induced chemical activation: Optimisation using surface response methodology. Chem. Eng. Res. Des. 91 (12), 2447–2456. Dec.

Hsi, H.C., Chen, C.T., 2012. Influences of acidic/oxidizing gases on elemental mercury adsorption equilibrium and kinetics of sulfur-impregnated activated carbon. Fuel 98, 229–235.

Jawad, A.H., Abdulhameed, A.S., 2020. Statistical modeling of methylene blue dye adsorption by high surface area mesoporous activated carbon from bamboo chip using KOH-assisted thermal activation. Energy, Ecol. Environ. 5 (6), 456–469. Dec.

Jawad, A.H., Mohd Firdaus Hum, N.N., Abdulhameed, A.S., Mohd Ishak, M.A., 2020. Mesoporous activated carbon from grass waste via H3PO4-activation for methylene blue dye removal: modelling, optimisation, and mechanism study. Int. J. Environ. Anal. Chem. 00, 1–17. Aug.

Jung, K.W., Choi, B.H., Song, K.G., Choi, J.W., 2019. Statistical optimization of preparing marine macroalgae derived activated carbon/iron oxide magnetic composites for sequestering acetylsalicylic acid from aqueous media using response surface methodologys. Chemosphere 215, 432–443. Jan.

Kacker, R.N., Lagergren, E.S., Filliben, J.J., 1991. Taguchi's orthogonal arrays are classical designs of experiments. J. Res. Natl. Inst. Stand. Technol. 96 (5), 577–591.

Khalili, S., Khoshandam, B., Jahanshahi, M., 2015. Optimization of production conditions for synthesis of chemically activated carbon produced from pine cone using response surface methodology for CO2 adsorption. RSC Adv 5 (114), 94115–94129.

A. Khuri and S. Mukhopadhyay, "Response Surface Experiments and Designs," in Handbook of Design and Analysis of Experiments, 1st ed., A. Dean, M. Morris, J. Stufken, and D. Bingham, Eds. CRC Press LLC, 2015, pp. 198–235.

Kiel, H.E., Sahaglan, J., Sundstrom, D.W., 1975. Kinetics of the Activated Carbon-Steam Reaction. Ind. Eng. Chem. Process Des. Dev. 14 (4), 470–473.

Leardi, R., 2009. Experimental design in chemistry: A tutorial. Anal. Chim. Acta 652 (1–2), 161–172.

Lillo-Ródenas, M.A., Cazorla-Amorós, D., Linares-Solano, A., 2003. Understanding chemical reactions between carbons and NaOH and KOH: An insight into the chemical activation mechanism. Carbon N. Y. 41 (2), 267–275.

Lim, A., Chew, J.J., Ngu, L.H., Ismadji, S., Khaerudini, D.S., Sunarso, J., 2020. Synthesis, Characterization, Adsorption Isotherm, and Kinetic Study of Oil Palm Trunk-Derived Activated Carbon for Tannin Removal from Aqueous Solution. ACS Omega 5 (44), 28673–28683. Nov.

Liu, J., Li, Y., Li, K., 2013. Optimization of preparation of microporous activated carbon with high surface area from Spartina alterniflora and its p-nitroaniline adsorption characteristics. J. Environ. Chem. Eng. 1 (3), 389–397. Sep.

Liu, Y., Ritter, J.A., 1998. Periodic State Heat Effects in Pressure Swing Adsorption-Solvent Vapor Recovery. Adsorption 4 (2), 159–172.

Loloei, Z., Soleimani, M., Mozaffarian, M., 2017. Optimisation of physical activation process for activated carbon production from tyre wastes. International Journal of Global Warming 11 (3), 358–372.

Loloie, Z., Mozaffarian, M., Soleimani, M., Asassian, N., 2017. Carbonization and CO2 activation of scrap tires: Optimization of specific surface area by the Taguchi method. Korean J. Chem. Eng. 34 (2), 366–375.

Loredo-Cancino, M., Soto-Regalado, E., Cerino-Córdova, F.J., García-Reyes, R.B., García-León, A.M., Garza-González, M.T., 2013. Determining optimal conditions to produce activated carbon from barley husks using single or dual optimization. J. Environ. Manage. 125, 117–125.

Mahmoodi, Z., Aghaie, H., Fazaeli, R., 2020. Application of response surface methodology for optimization of cadmium removal by Aloe Vera/carboxylated carbon nanotubes nanocomposite-based low-cost adsorbent. Mater. Res. Express 7 (6), 65015. Jun.

Makeswari, M., Santhi, T., 2013. Optimization of preparation of activated carbon from Ricinus communis leaves by microwave-Assisted zinc chloride chemical activation: Competitive adsorption of Ni 2+ ions from aqueous solution. J. Chem.

Md-Desa, N.-S., Ab Ghani, Z., Abdul-Talib, S., Tay, C.-C., 2016. OPTIMIZATION OF ACTIVATED CARBON PREPARATION FROM SPENT MUSHROOM FARMING WASTE (SMFW) VIA BOX-BEHNKEN DESIGN OF RESPONSE SURFACE METHODOLOGY (Penyediaan Secara Optimum Arang Teraktif daripada Sisa Tanaman Cendawan. Malaysian J. Anal. Sci. 20, 461–468.

Miller, S.J., Dunham, G.E., Olson, E.S., Brown, T.D., 2000. Flue gas effects on a carbon-based mercury sorbent. Fuel Process. Technol. 65, 343–363.

Montgomery, D., 2017. Design and Analysis of Experiments, 8th ed. John Wiley & Sons, Incorporated.

Mozaffarian, M., Soleimani, M., Bajgiran, M.A., 2019. A simple novel route for porous carbon production from waste tyre. Environ. Sci. Pollut. Res. 26 (30), 31038–31054. Oct.

Muzic, M., Sertic-Bionda, K., Gomzi, Z., Podolski, S., Telen, S., 2010. Study of diesel fuel desulfurization by adsorption. Chem. Eng. Res. Des. 88 (4), 487–495.

O'Mahony, T., Guibal, E., Tobin, J.., 2002. Reactive dye biosorption by Rhizopus arrhizus biomass. Enzyme Microb. Technol. 31 (4). Sep.

Pereira Da Silva, C., Da Guarda Souza, M.O., Dos Santos, W.N.L., Oliveira Bastos Silva, L., 2019. Optimization of the Production Parameters of Composites from Sugarcane Bagasse and Iron Salts for Use in Dye Adsorption. Sci. World J. 2019.

Pledger, K., 2008. Normal distribution. Modular Mathematics. Edexcell, p. 177.

Ramalingam, S.G., et al., 2011. Hazardous dichloromethane recovery in combined temperature and vacuum pressure swing adsorption process. J. Hazard. Mater. 198, 95–102.

Ramalingam, S.G., et al., 2012. Different families of volatile organic compounds pollution control by microporous carbons in temperature swing adsorption processes. J. Hazard. Mater. 221–222, 242–247.

Rashidi, N.A., Yusup, S., 2015. Effect of process variables on the production of biomass-based activated carbons for carbon dioxide capture and sequestration. Chem. Eng. Trans. 45, 1507–1512.

Rashidi, N.A., Yusup, S., 2019. Production of palm kernel shell-based activated carbon by direct physical activation for carbon dioxide adsorption. Environ. Sci. Pollut. Res. 26 (33), 33732–33746.

Rashidi, N.A., Yusup, S., Hameed, B.H., 2013. Kinetic studies on carbon dioxide capture using lignocellulosic based activated carbon. Energy 61, 440–446.

Rio, S., Faur-Brasquet, C., Coq, L.Le, Courcoux, P., Cloirec, P.Le, 2005. Experimental design methodology for the preparation of carbonaceous sorbents from sewage sludge by chemical activation - Application to air and water treatments. Chemosphere 58 (4), 423–437.

Rodríguez-Mosqueda, R., Bramer, E.A., Roestenberg, T., Brem, G., 2018. Parametrical Study on CO2 Capture from Ambient Air Using Hydrated K2CO3 Supported on an Activated Carbon Honeycomb. Ind. Eng. Chem. Res. 57 (10), 3628–3638.

Saberimoghaddam, A., Nozari, A., 2017. An experimental and statistical model of a cyclic pressure swing adsorption column for hydrogen purification. Korean J. Chem. Eng. 34 (3), 822–828.

Smallwood, H.M., 1947. Design of Experiments in Industrial Research. Anal. Chem. 19 (12), 950–952.

Snetsinger, P., Alkhatib, E., 2018. Flexible Experiment Introducing Factorial Experimental Design. J. Chem. Educ. 95 (4), 636–640.

Subramaniam, R., Kumar Ponnusamy, S., 2015. Novel adsorbent from agricultural waste (cashew NUT shell) for methylene blue dye removal: Optimization by response surface methodology. Water Resour. Ind. 11, 64–70. Sep.

Suzuki, T., Kawamura, H., Yasui, S., Ojima, Y., 2012. Proposal of Advanced Taguchi's Linear Graphs for Split-Plot Experiments. Frontiers in Statistical Quality Control 10. Physica-Verlag HD, Heidelberg, pp. 339–348.

Tan, I.A.W., Ahmad, A.L., Hameed, B.H., 2008. Optimization of preparation conditions for activated carbons from coconut husk using response surface methodology. Chem. Eng. J. 137 (3), 462–470. Apr.

Vohra, M., Al-Suwaiyan, M., Hussaini, M., 2020. Gas phase toluene adsorption using date palm-tree branches based activated carbon. Int. J. Environ. Res. Public Health 17 (24), 1–19.

Vohra, M.S., 2015. Adsorption-Based Removal of Gas-Phase Benzene Using Granular Activated Carbon (GAC) Produced from Date Palm Pits," Arab. J. Sci. Eng. 40 (11).

Wanjeri, V.W.O., Gbashi, S., Ngila, J.C., Njobeh, P., Mamo, M.A., Ndungu, P.G., 2019. Chemical vapour deposition of MWCNT on silica coated Fe3O4 and use of response surface methodology for optimizing the extraction of organophosphorus pesticides from water. Int. J. Anal. Chem. 2019.

Yu, P., et al., 2020. Activated carbon-based CO2uptake evaluation at different temperatures: The correlation analysis and coupling effects of the preparation conditions. Journal of CO2 Utilization 40.